Preroughening transitions in crystal surfaces and valence-bond phases in quantum spin chains

Marcel den Nijs
Department of Physics, FM-15, University of Washington, Seattle, Washington 98195

Koos Rommelse
Department of Theoretical Physics, University of Oxford, 1 Keble Road, Oxford OX1 3NP, United Kingdom
(Received 10 April 1989)

We show that disordered flat phases in crystal surfaces are equivalent to valence-bond-type phases in integer and half-integer spin quantum chains. In the quantum spin representation the disordered flat phase represents a fluid-type phase with long-range antiferromagnetic spin order. This order is stabilized dynamically by the hopping of the particles and short-range spin-exchange interactions. The mass of Néel solitons is finite. Numerical finite-size-scaling results confirm this. We identify the order parameter of the valence-bond phase. The Haldane conjecture suggests a fundamental difference between half-integer and integer antiferromagnetic Heisenberg spin chains. We find that disordered flat phases are realized in both cases, have exactly the same type of long-range antiferromagnetic spin order, and are stabilized by exactly the same mechanism. They differ only in the mathematical formulation of broken symmetry in the spin representation. We suggest experimental methods of observing disordered flat phases in crystal surfaces.

I. INTRODUCTION

Spin quantum chains have been a focus of research for many years. In 1983 Haldane[1] predicted that, contrary to the spin-$\frac{1}{2}$ chain, the spin-1 chain is not massless at its isotropic Heisenberg antiferromagnetic (HAF) point but is in a phase with a finite-mass gap, different from the Néel phase with long-range antiferromagnetic (AF) order. More generally, he predicted that all AF isotropic Heisenberg chains with integer spin s are massive. Half-integer chains are expected to be massless at their HAF point. This prediction is based on a mapping of the spin chains in the limit of large s onto the nonlinear σ model.

Subsequently, numerous numerical calculations have checked this mass gap for the $s=1$ case.[2] Although controversial at first, it is now commonly agreed that the numerical evidence supports the conjecture. Last year Affleck *et al.*,[3] followed by others,[4] suggested that the ground state has a valence-bond solid (VBS) character. They showed that at a special point in the phase diagram of the spin-1 chain, not too far from the HAF point, the exact ground state can be written as a VBS state. This result has triggered general interest in quantum spin chains because VBS states have a Jastrow wave-function structure[4] and therefore striking similarities with the Laughlin wave function used to explain the fractional quantum Hall effect.[5] Moreover, VBS states are proposed to explain high-T_c superconductivity.[6]

In this paper we show that the disordered flat (DOF) phase which we discovered earlier in the context of the statistical mechanics of two-dimensional (2D) surface-roughening transitions[7] is equivalent to these VBS-type phases in 1D quantum chains. The virtue of this equivalence is that it provides simple physical insight into the nature of the ground state in VBS phases, the mechanism that stabilizes them, and it allows us to identify the correlation functions, order parameters, and particle and soliton masses (interface free energies) that distinguish this phase from the other phases.

We will interpret spin-s chains for integer spin s as diluted spin-$(s-\frac{1}{2})$ chains. The site is empty, the $S_n^z=0$ state, or occupied by a spin-$(s-\frac{1}{2})$ particle, with the states $S_n^z=\pm1,\pm2,\ldots\pm s$ representing the spin of the particle.

These particles form a solid, fluid, or dilute gas with or without long-range AF spin order in various regions of the phase diagram. We will show that they form a fluid with long-range antiferromagnetic (AF) spin order in the VBS phase. This interpretation elucidates the properties of the spin-s chain and VBS phases considerably because it is close to the statistical mechanical crystal surface representation of the model. The steps in crystal surface configurations are the world lines of these spin-$(s-\frac{1}{2})$ particles.

VBS phases are not disordered; they have long-range AF spin order, similar to the Néel phase (the solid phase with AF spin order), but the positional disorder of the particles in the DOF phase makes it more difficult to identify the order. We define the order parameter of the VBS phase in Sec. IV, show that Néel solitons have a finite mass in the DOF phase, and calculate this soliton mass numerically by finite-size scaling.

In Sec. II we review the properties of the DOF phase in crystal surfaces and the mechanism that stabilizes it. We give a simple, but general, entropy argument, followed by a more detailed argument that uses a decomposition of the restricted solid-on-solid (RSOS) model into an Ising model and a six-vertex model. The latter elucidates the structure of the RSOS model phase diagram.[7] We introduce order parameters, correlation functions,

and interface free energies that distinguish between the rough, the DOF, and the flat crystal phases. We determine the scaling properties of the preroughening transition and the locations of the phase boundaries between the DOF, flat, and rough crystal phases in the RSOS model numerically from the finite-size-scaling behavior of these interface free energies. Finally we suggest methods to observe preroughening and DOF phases experimentally.

In Sec. III we discuss the equivalence between the 2D RSOS model and the spin-1 quantum chain, using the transfer matrix formalism. In the RSOS model the steps in the surface are restricted to height changes $\delta h = 0, \pm 1$. More generally, solid-on-solid (SOS) models where the steps are restricted to $\delta h = 0, \pm 1, \pm 2, \ldots \pm s$ are equivalent to integer spin-s chains. Half-integer spin chains are equivalent to body-centered solid-on-solid (BCSOS) models that describe the roughening of surfaces with a body-centered-type structure.

In Sec. IV we discuss the phase diagram of the spin-1 quantum chain. The spin-1 chain corresponds to the RSOS model in the very anisotropic lattice limit. Therefore, the structure of its phase diagram is identical to that of the RSOS model on an isotropic lattice (Sec. II). We repeat the explanation of this structure, but now from the perspective of the spin-1 chain as a diluted spin-$\frac{1}{2}$ chain. The spin-$\frac{1}{2}$ particles form a solid, fluid, or gas, with or without long-range order of their spins: the flat crystal surface phase represents the dilute gas phase (the disordered singlet phase); the DOF phase represents a fluid with AF ordered spins (the VBS phase); the RSOS rough phase represents a fluid phase with massless spin wave excitations; the BCSOS flat phase represents a solid with long-range AF spin order (the Néel phase); the BCSOS stepped phase [where the surface decomposes into (1,1) and (1,−1) facets] represents a solid with long-range ferromagnetic ordered spins; and finally, the BCSOS rough phase represents a solid with massless spin-wave excitations. Next, we translate the correlation functions, order parameters, and interface free energies, of Sec. II, that distinguish between the VBS phase and these other phases into the spin-1 formulation, and present additional numerical evidence confirming our identification of the VBS phase.

In Sec. V we discuss the connection between the VBS state and the DOF phase. Affleck *et al.*[3] discovered that the VBS state is the ground state at a point in the phase diagram of the spin-1 chain, not too far from the Heisenberg AF (HAF) point. They expect it to be a good approximation of the ground state at the HAF point. We show that the VBS ground state exhibits the properties of the DOF phase. The spin-$\frac{1}{2}$ particles are placed completely at random in the VBS state, but maintain perfect long-range AF spin order. The positional disorder is maximal and the AF spin order is perfect. The VBS state is the prototype state for the DOF phase. From the renormalization transformation point of view, the exactly soluble VBS point must play the role of fixed point of the DOF phase (all the points inside the DOF phase must flow to it under scale transformations).

In the diluted spin-$\frac{1}{2}$ formulation the VBS ground state obtains the character of a noninteracting lattice gas. This simplifies the calculation of the correlation functions to the extent that they become trivial. We evaluate all the correlation functions and interface free energies defined in Secs. II and IV at the VBS point.

In Sec. VI we discuss the differences between integer and half-integer spin chains. The Haldane conjecture is often paraphrased as stating that in integer spin chains the HAF point is massive, and in half-integer spin chains massless. This seems to say that DOF phases are absent in half-integer spin chains, which contradicts physical intuition. Half-integer spin chains are equivalent to body-centered solid-on-solid (BCSOS) models, that describe the roughening of crystal surfaces with a body-centered-type structure. DOF phases must be realized in these surfaces as well according to our general entropy argument presented in Sec. II. There can be no fundamental difference between SOS models and BCSOS models, i.e., integer and half-integer spin chains.

It is no surprise that the exact soluble spin-$\frac{1}{2}$ chain, does not exhibit a DOF phase; the HAF point belongs to the rough phase.[8] The interactions are restricted to nearest neighbors. The steps in the BCSOS model are composite objects, i.e., $\uparrow\uparrow$ and $\downarrow\downarrow$ excitations with respect to the perfectly ordered Néel ground state. Therefore, according to our discussion in Sec. II, the interactions between the spins do not have enough range to stabilize a DOF phase.

Indeed, if we extend the range of the interactions, we find a DOF phase. In Sec. VI we show that the VBS ground state at the exactly soluble spin-$\frac{1}{2}$ point of Majumdar and Ghosh[9] belongs to the DOF phase. This VBS state plays the role of the prototype DOF state (the fixed point of the DOF phase), in analogy with the VBS ground state in the spin-1 chain. Steps are placed again completely at random, but maintain perfect AF order.

The only difference between DOF phases in the half-integer and integer spin representation is the presence and absence, respectively, of a ground-state degeneracy conjugate to this long-range order. The ground state is twofold degenerate in DOF phases in half-integer spin chains, but nondegenerate in integer spin chains (Sec. VI). This is a peculiarity of the quantum spin formulation. The DOF phase (and also the flat crystal phase) has a conventional ground-state degeneracy, a spontaneously broken symmetry, and a local order parameter in both the SOS and BCSOS model (Sec. II). However, in the spin-1 formulation we lose knowledge of the absolute height of the crystal surface (the surface configuration is represented by the steps in the surface), and as a result we lose the ground-state degeneracy of the DOF phase (and also of the RSOS flat phase). This suggests that in the spin-1 formulation the DOF phase obtains the semimysterious property of being a fluid state with long-range order without a ground-state degeneracy. In the spin-1 representation we can still calculate the absolute value of its order parameter (it becomes a string operator), but not its sign. This type of long-range order is known as off-diagonal long-range order in the quantum Hall effect.[10]

On the other hand, the crystal surface is corrugated in body-centered-type surfaces. This implies a twofold de-

generacy of the ground state of the DOF phase (and also of the BCSOS flat phase) in half-integer spin chains. This degeneracy couples to the parity of the height of the surface (i.e., whether the average height of the surface is an even or odd integer plus $\frac{1}{2}$). The corrugation of the surface in the BCSOS model acts like a local variable that keeps track of the parity of the average height of the surface. This aspect is sufficient to be able to express the order parameters of the BCSOS flat and DOF phase in terms of local spin operators.

In the final analysis the content of the Haldane conjecture is quite limited. DOF phases are realized in integer and half-integer spin chains alike. They have exactly the same type of long-range order, are stabilized by exactly the same physical mechanism, have exactly the same properties, and the phase diagrams of integer and half-integer spin chains look alike. The only difference is that in half-integer spin chains the long-range AF order of the "spins" (the $\uparrow\uparrow$ and $\downarrow\downarrow$ excitations with respect to the perfectly ordered Néel ground state) can be expressed in terms of a local order parameter, while in integer-spin chains this information is lost.

II. DISORDERED FLAT PHASES IN CRYSTAL SURFACES

A. Surface roughening

The roughening of crystal surfaces is conventionally described by solid-on-solid (SOS) models.[11] The surface is characterized by means of integer-valued column height variables $h_{\mathbf{r}}$ defined on a two-dimensional lattice. We consider the so-called restricted solid-on-solid (RSOS) model, which is the special SOS model where nearest-neighbor columns $\mathbf{r}$ and $\mathbf{r}'$ are allowed to differ by at most 1, $h_{\mathbf{r}}-h_{\mathbf{r}'}=0, \pm 1$. In other words, where only steps of height 1 are allowed.

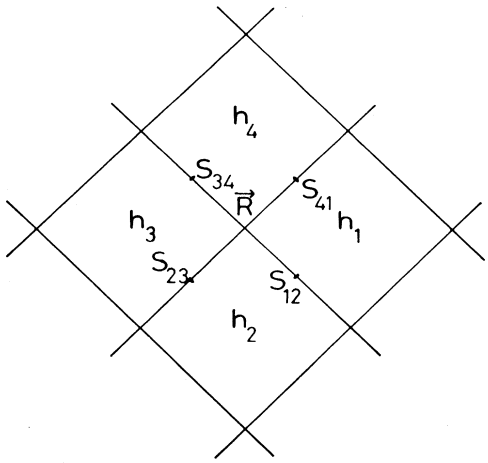

FIG. 1. Rectangular lattice with column heights h_i, step variables $S_{i,j}$, and vertices $\mathbf{R}$.

The most general RSOS model Hamiltonian with interactions between the four heights h_1, h_2, h_3, and h_4, around each vertex $\mathbf{R}$, see Fig. 1, can be written as[12]

$$H_{\mathrm{RSOS}}=\sum_{R}\{K[\delta(|h_1-h_2|-1)+\delta(|h_2-h_3|-1)]+L_1^{(x)}\delta(|h_1-h_3|-1)+L_2^{(x)}\delta(|h_1-h_3|-2)$$
$$+L_1^{(t)}\delta(|h_2-h_4|-1)+L_2^{(t)}\delta(|h_2-h_4|-2)+Q\delta(|h_1-h_3|-1)\delta(|h_2-h_4|-1)\}\ , \tag{2.1}$$

with $\delta(x)=1$ for $x=0$ and $\delta(x)=0$ for $x\neq 0$. All energies are measured in units of $1/k_BT$, and we have chosen a square lattice. Throughout this section the interactions are isotropic, $L_1^{(x)}=L_1^{(t)}$ and $L_2^{(x)}=L_2^{(t)}$, but this is not essential, and in the following sections anisotropy will play an important role. Figure 2 shows the phase diagram of the RSOS model in the (K,L_2) subspace with $Q=L_1=0$.

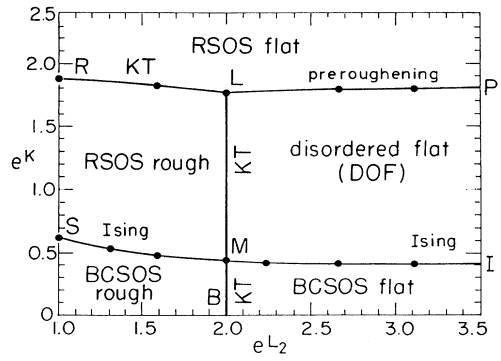

FIG. 2. Phase diagram of the RSOS model with nearest-neighbor interactions K and step repulsion $L_2=L_2^{(x)}=L_2^{(t)}$, and the coupling constants $Q=L_1^{(x)}=L_2^{(t)}=0$.

First we summarize briefly the conventional roughening theory, as realized, e.g., in models with only nearest-neighbor interactions (along the K axis in Fig. 2). At low temperatures ($K\gg 0$) the surface is flat. It contains a few thermodynamically excited terraces where the surface is higher or lower (by one unit); see Fig. 3(a). Thermodynamic excitations are of order k_BT. The free energy of a terrace is proportional to its step length $\pi\xi$. ξ is the average terrace diameter and is proportional to the correlation length. We measure all free energies in units

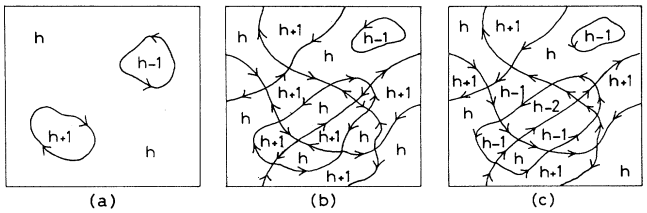

FIG. 3. Typical configurations in the RSOS flat phase (a), the disordered flat (DOF) phase (b), and RSOS rough phase (c).

of $k_B T$. Therefore the terrace size and step free energy η are related as $\pi\xi\eta \simeq 1$. At low temperatures these terraces are small and few, but their number and typical size increases with temperature. At first, meander entropy is the dominant factor in reducing the step free energy, until reaching temperatures where the terraces start to communicate with each other. From there on the topological rules that govern how steps can intertwine and the symmetries associated with the short-range interactions between steps become the limiting factors in the increase in entropy. As always, these topological rules and symmetries determine the universality class of the transition.

At high temperatures, in the rough phase about $K=0$, the surface resembles a terraced mountainlike landscape; see Fig. 3(c). At large length scales the discreteness of the step heights has become irrelevant, and the surface can be described by the Gaussian model.[11] In other words, it has the same properties as a transverse vibrating elastic network. The free energy of the capillary waves is gapless. The surface is fully characterized by the so-called roughness parameter, K_g^{-1}, which is the inverse of the coupling constant of this effective Gaussian model. The height-height correlations diverge logarithmically with an amplitude proportional to the roughness parameter,

$$\langle (h_{\mathbf{r}} - h_{\mathbf{r}'})^2 \rangle \simeq \frac{1}{\pi K_g} \ln(r) . \tag{2.2}$$

Conventionally, the transition between the flat and rough phases is a single transition, and belongs to the Kosterlitz-Thouless (KT) universality class.[11] At the KT transition the roughness parameter takes the universal value $K_g = \pi/2$. This has been well established numerically[11,13] and also experimentally,[14,15] but most of this earlier numerical work was restricted to SOS models with only nearest-neighbor interactions.

B. Disordered flat phases

The above conventional scenario applies when the hard-core repulsion part of the interactions between the steps dominates. We found a new phase in between the rough and flat crystal phase by simply increasing the range of the interactions in the RSOS model.[7] We named this new phase the disordered flat (DOF) phase because the surface remains flat on average although it contains a disordered array of steps.[7] The step free energy has already vanished, but the steps have long-range up-down-up-down order. Figure 3(b) shows a typical configuration. The steps are disordered positionally but up and down steps alternate. Beyond the multicritical point L in Fig. 2 the transition takes place in two stages: first the preroughening transition between the flat and DOF phase, followed by the roughening transition between the DOF and rough phase.

It is advantagous to characterize the configurations of the crystal surface by steps instead of column heights. The steps form closed loops. They follow the bonds of lattice $\mathcal{D}$, dual to the lattice formed by the sites of the height variables, $\mathcal{L}$. Associate a step variable

$$S_{\mathbf{r},\mathbf{r}'} = h_{\mathbf{r}} - h_{\mathbf{r}'} = 0, \pm 1$$

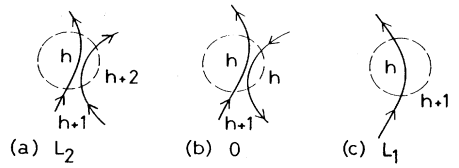

FIG. 4. Repulsive (L_2) and attractive (L_1) interactions between steps originating from further-than-nearest-neighbor interactions between the column heights. The dashed circle denotes the interaction range.

with each bond of $\mathcal{D}$. It is important to distinguish between up and down steps, because $S_{\mathbf{r},\mathbf{r}'} = -S_{\mathbf{r}',\mathbf{r}}$. In Fig. 3 we denote this by placing arrows along the steps. In the direction along the arrow the height to the left of the step is (one unit) lower. At each intersection of steps the flux of arrows must be equal to zero, because $\sum_{\mathcal{L}} S_{\mathbf{r},\mathbf{r}'} = 0$ along every closed contour of lattice $\mathcal{L}$. Later, in Secs. III–V, these step variables become quantum spins. In the DOF phase the steps, $S_{\mathbf{r},\mathbf{r}'} = \pm 1$ states, have long-range AF order but are positionally disordered.

The DOF phase is stabilized by a combination of step entropy and step interactions. Nearest-neighbor (NN) interactions are blind to the arrows. They contribute only to the step energy. Further-than-NN interactions, like L_1 and L_2 in the RSOS model, look across more than one step. L_2 represents a short-range repulsion between steps with parallel arrows and L_1 a short-range attraction between steps with opposite arrows; see Fig. 4. Consider the extreme case where the repulsion is infinitely strong, $L_2 \to \infty$, and attraction is absent, $L_1 = 0$. Steps with parallel arrows are forbidden to approach each other closer than the interaction range, while steps with antiparallel arrows can approach each other at will. The steps have more meander entropy in configurations where the steps have alternating up-down-up order [Fig. 5(a)] than in configurations where neighboring steps have parallel arrows [Fig. 5(b)]. This shows that the DOF structure is favored by a combination of entropy and further-than-nearest-neighbor interactions.

Notice that these further-than-nearest-neighbor interactions are simply ferromagnetic [not competing ones

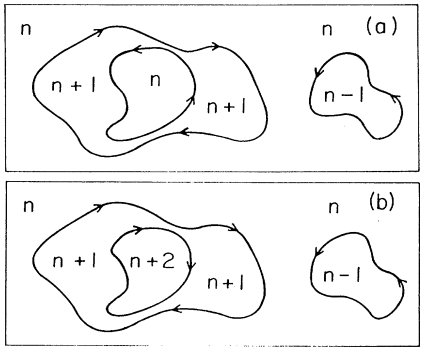

FIG. 5. Surface configurations with nested up-down steps (a) and up-up steps (b).

as in, e.g., the axial next-nearest-neighbor Ising model[16], and that they must be a common feature of experimental systems. Also notice that this entropy effect plays a role only at temperatures high enough such that the terraces intertwine.

C. Diluted six-vertex model representation

This argument is general, independent of the SOS model description, but is not conclusive because it does not tell whether the effect is strong enough to stabilize the long-range AF step order of the DOF phase. A stronger argument is obtained by rewriting the RSOS model as an Ising model coupled to a six-vertex model.[7] Assign an Ising spin $\sigma_r=\pm 1$ to each column height: $\sigma_r=\exp(i\pi h_r)$. It represents the parity of the column height. An Ising Bloch wall represents the presence of a step between two nearest-neighbor columns. We introduce a six-vertex model on the lattice formed by the Ising-Bloch walls to represent whether a step is up or down. We multiply the Boltzmann weight of each Ising configuration with the partition function of a six-vertex model defined on the Ising-Bloch wall lattice. This is a trace over all arrow configurations on the Ising-Bloch walls such that at each Bloch wall intersection the flux of the arrows is equal to zero. In this formulation the RSOS model partition function reads

$$Z_{\mathrm{RSOS}}=\sum_{\{\sigma_r\}}\exp[-H_I(K,L_1^{(x)},L_1^{(t)},Q)] \times Z_{\text{six-vertex}}(\{\sigma_r\},L_2^{(x)},L_2^{(t)}) , \tag{2.3a}$$

with

$$H_I=\sum_R[\tfrac{1}{2}K(1-\sigma_1\sigma_2)+\tfrac{1}{2}K(1-\sigma_2\sigma_3)+\tfrac{1}{2}L_1^{(x)}(1-\sigma_1\sigma_3) +\tfrac{1}{2}L_1^{(t)}(1-\sigma_2\sigma_4)+\tfrac{1}{4}Q(1-\sigma_1\sigma_3)(1-\sigma_2\sigma_4)] . \tag{2.3b}$$

It is a bond diluted six-vertex model on a lattice that is not rigid but has annealed fluctuations in its shape and number of bonds. At all times the lattice shape remains compatible with long-range AF arrow order because every Ising-Bloch wall lattice can be interpreted as an array of closed loops and therefore maintains the two-sublattice structure essential for unfrustrated AF arrow order.

It is noteworthy that the six-vertex model serves as a model for surface roughening in its own right. It is equivalent to the so-called body-centered solid-on-solid (BCSOS) model,[17] which describes surfaces with a body-centered type of structure such as (110) faces of fcc crystals like Cu and Ni. The atoms in the next layer are not placed on top of those in the previous layer, but above the plaquettes (see Fig. 6). In the BCSOS model this is modeled by assigning even values of the column heights to one sublattice and odd values to the other sublattice, i.e., by demanding that all nearest-neighbor columns

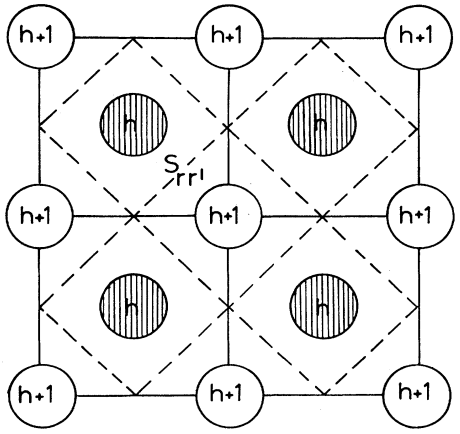

FIG. 6. Atom configuration in body-centered-type surfaces, and definition of step variables $\delta h=S_{i,j}=\pm 1$ in the BCSOS model.

differ in height by one, $h_r-h_{r'}=\pm 1$. When formulated in terms of step variables this leads immediately to the six-vertex model.

D. Phase diagram of the RSOS model

Equation (2.3) clarifies the general structure of the phase diagram of the RSOS model, Fig. 2. The coupling constants K, L_1^x, L_1^t, and Q govern the Ising-type order. They control the density and positional order of the steps (the vertical direction in Fig. 2). The coupling constants L_2^x and L_2^t govern the six-vertex-type order. They represent the conventional interactions between arrows at intersections in the six-vertex model [see Fig. 7(a)]. They control the long-range AF order in the steps (the horizontal direction in Fig. 2).

The Ising spins are antiferromagnetically (AF) ordered

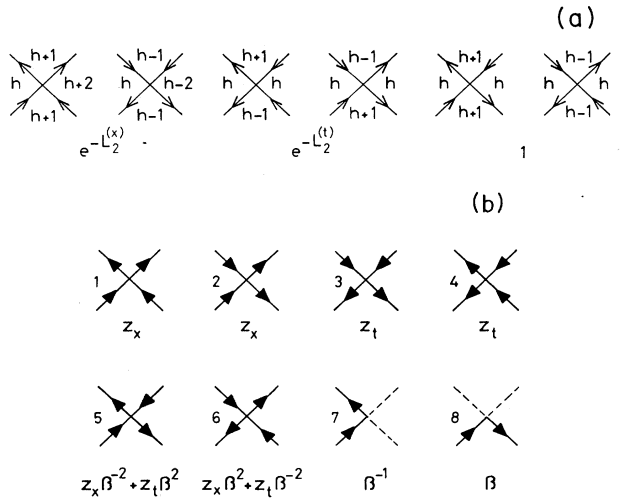

FIG. 7. (a) Conventional Boltzmann weights in the six-vertex model. (b) Boltzmann weights of the six-vertex model equivalent to the polygon problem (defined in the Appendix).

in the limit $K \to -\infty$, see Fig. 2. Each bond contains an Ising-Bloch wall. The model reduces to the exactly soluble six-vertex model on a square lattice.[8] Each bond is occupied by an up or down step. From the exact solution it follows that for

$$\exp(-L_2^{(x)})+\exp(-L_2^{(t)})<1$$

the arrows have long-range AF order. This is the BCSOS flat phase. The column heights alternate between two values. For

$$\exp(-L_2^{(x)})+\exp(-L_2^{(t)})>1$$

the arrows are disordered, but with massless spin-wave excitations. This is the BCSOS rough phase where the steps form valleys and mountains on all length scales. The roughening transition takes place at

$$\exp(-L_2^{(x)})+\exp(-L_2^{(t)})=1$$

and is a KT transition.

The Ising spins remain AF ordered for finite values of $K \ll 0$. The Bloch walls still form a square array, but with missing bonds (closed loops) at length scales smaller than the Ising correlation length (see Fig. 8). Such imperfections cannot change the long-distance behavior of the BCSOS rough and flat phases, nor the universality class of the roughening transition. However, the missing bond excitations renormalize the roughness parameter of the BCSOS rough phase. They reduce the roughness of the surface. Numerical results along the K axis confirm this.[18] However, surprisingly, they do not renormalize the roughness parameter in the direct vicinity of the KT transition; we find that the KT transition line is exactly located at

$$\exp(-L_2^{(x)})+\exp(-L_2^{(t)})=1$$

for finite values of K up to point L (see also the Appendix).

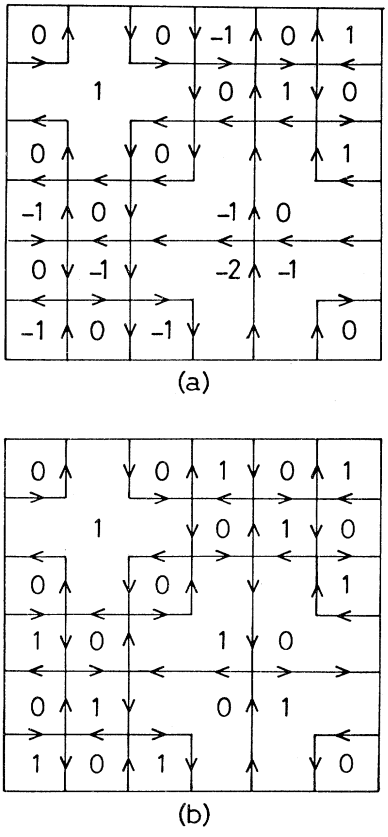

FIG. 8. Surface configurations in the BCSOS rough phase (a) and BCSOS flat phase (b).

The Ising spins disorder along the AF Ising critical line S-M-I (see Fig. 2). Only the Ising type of degrees become critical. Therefore this transition line must belong to the conventional Ising universality class (except at the multicritical point M). The only effect of the critical fluctuations of the Ising spins on the roughening degrees of freedom is a logarithmic singularity in the roughness parameter along the S-M segment inside the rough phase.[18]

The Ising spins must be disordered for $K \approx 0$. The Ising-Bloch walls form a disordered array. For increasing K this array contains an increasing number of disconnected finite pieces, but it always includes one infinitely large connected backbone cluster. This backbone cluster must exist, because otherwise the Ising spins would have long-range ferromagnetic order. Consider one specific Ising-Bloch wall configuration. Each finite cluster acts as an independent six-vertex model. Its arrows are disordered for all values of L_2, because finite systems cannot maintain long-range order. So the six-vertex model defined on the backbone cluster is solely responsible for the long-range order in the DOF phase. In general the universality class of a phase transition does not change with the shape of the underlying lattice. Therefore the six-vertex model on the backbone should undergo a conventional roughening transition. Its rough phase at small values of L_2 represents the conventional rough phase of the RSOS model [Fig. 3(c)]. Its flat phase at large values of L_2 represents the DOF phase [Fig. 3(b)]. This establishes the long-range order of the DOF phase: the surface contains a disordered array of steps, but remains flat on average because the height fluctuations are limited by the long-range AF arrow order on the backbone.

The backbone disintegrates, along the critical line R-L-P. The Ising and six-vertex type of degrees of freedom become critical simultaneously. Therefore this transition does not belong to the Ising model universality class. For small values of L_2, along the RSOS rough segment R-L, it is a KT transition. This follows from the conventional KT renormalization theory for SOS models.[11] At large values of L_2, along the DOF segment L-P, this is the novel preroughening transition which we introduced earlier.[7]

The Ising spins have ferromagnetic long-range order for $K \gg 0$, beyond the critical line R-L-P. This is the RSOS flat phase [see Fig. 3(a)]. The six-vertex lattice has fallen apart completely. Only finite Ising-Bloch wall lattices (disconnected terraces) remain. On each the six-vertex arrows are disordered for all finite values of L_2.

The surface is flat because each of these finite disordered six-vertex models represents only a local excitation with respect to the infinitely large cluster of ferromagnetically ordered Ising spins, which has taken over the role of infinite backbone, that keeps the height fluctuations finite.

A convenient way to summarize the structure of the phase diagram is to view it as a superposition of the conventional phase diagram of the Ising model with interactions K, L_1^x, L_1^t, and Q,[19] and the phase diagram of the six-vertex model with interactions L_2^x and L_2^t.[8] Most of the transitions in the phase diagram are driven by only the Ising or only the six-vertex degrees of freedom and therefore retain their conventional type of scaling behavior and critical exponents. The KT transition line R-L and the preroughening transition line L-P (they replace the ferromagnetic critical line of the conventional Ising model), and the isolated multicritical point M are the only exceptions.

For the stability of the DOF-type long-range order it is essential that the backbone cluster of Ising-Bloch walls has dimensionality $D=2$. It must span the entire lattice like a percolating network because a finite lattice cannot maintain long-range order. The fluctuations and random shape of the backbone does not matter because the lattice remains compatible with the AF long-range arrow order at all times. It is also important that the spatial fluctuations in the lattice cutoff are bounded by the Ising correlation length. It is likely that all these conditions are satisfied. Moreover, our numerical results discussed below confirm it. It is possible to visualize more complicated types of phases, for example, DOF phases where the arrows have a higher order periodicity.[20] We have no positive evidence for the presence of such generalized DOF phases in Fig. 2. Our numerical results leave room for it in the vicinity of the multicritical point L, but the slow numerical convergence that we encounter there is consistent with the expected interference between preroughening and KT roughening.

E. Order parameters

It is important to define order parameters that distinguish between the DOF phase and the other phases. Consider the spin-spin correlation function of the Ising degrees of freedom (the parity of the column heights),

$$G_H(\mathbf{r}_n-\mathbf{r}_0)=\langle\sigma_{\mathbf{r}_n}\sigma_{\mathbf{r}_0}\rangle=\langle\exp[i\pi(h_{\mathbf{r}_n}-h_{\mathbf{r}_0})]\rangle\ . \tag{2.4}$$

The Ising spins are disordered in the DOF phase and the RSOS rough phase, but ordered in the RSOS flat phase. G_H decays exponentially to zero in the DOF phase and to zero as a power law in the RSOS rough phase, but decays exponentially to the square of the Ising magnetization,

$$\rho=\langle\exp(i\pi h_{\mathbf{r}})\rangle\ , \tag{2.5}$$

in the RSOS flat phase. The Ising spins are AF ordered in the BCSOS flat and rough phase. There, G_H decays exponentially to the square of the staggered magnetization

$$\rho_s=\langle\exp[i\pi(x+y+h_{\mathbf{r}})]\rangle\ , \tag{2.6}$$

with x and y the coordinates of the sites on the square lattice, $\mathbf{r}=(x,y)$.

Consider the step-step correlation function

$$G_s(\mathbf{r}_n-\mathbf{r}_0)=\langle(h_{\mathbf{r}_n}-h_{\mathbf{r}'_n})\exp[i\pi(h_{\mathbf{r}_n}-h_{\mathbf{r}_0})](h_{\mathbf{r}_0}-h_{\mathbf{r}'_0})\rangle\ , \tag{2.7}$$

where $\mathbf{r}'_n$ a nearest-neighbor site to the left (above) site $\mathbf{r}_n$ on the square lattice. The phase factor contributes a plus (minus) sign to the correlation function when the height difference between sites $\mathbf{r}_n$ and $\mathbf{r}_0$ is even or odd. The steps have long-range AF arrow order in the DOF phase, and also in the BCSOS flat phase. The steps have predominantly parallel (antiparallel) arrows if this height difference is even (odd). G_s decays exponentially to zero in the RSOS flat phase, and to zero as a power law in the RSOS rough phase, but exponentially to the square of the order parameter

$$\psi=\langle\exp(i\pi h_{\mathbf{r}})(h_{\mathbf{r}}-h_{\mathbf{r}'})\rangle \tag{2.8}$$

in the DOF and BCSOS flat phases.

These three order parameters allow us to distinguish between the DOF phase and the other phases: in the RSOS flat phase only ρ is nonzero; in the DOF phase only ψ is nonzero; and in the BCSOS flat phase both ψ and ρ_s are nonzero. Conjugate to these three order parameters are three types of interfaces. They are the focus of our numerical work.

Consider an ensemble where the average height is fixed, e.g., by fixing the total number of particles. Suppose that the global average height is an integer, $\langle h\rangle=n$. The RSOS flat phase contains one single phase. The average height is a half-integer in the DOF phase. Therefore, the surface phase separates into DOF phases with average height $\langle h\rangle=n+\frac{1}{2}$ and $\langle h\rangle=n-\frac{1}{2}$. The order parameter ψ, Eq. (2.8), changes sign across the Néel-type interface between these phases. This type of interface consists of a neighboring pair of steps with parallel arrows.

The opposite happens when the global average height is fixed to be a half integer, $\langle h\rangle=n+\frac{1}{2}$. Now the DOF phase contains a single phase, and phase-separation occurs at the RSOS flat side. RSOS flat phases with average height $\langle h\rangle=n$ and $\langle h\rangle=n+1$ coexist, separated by interfaces where the order parameter ρ, Eq. (2.5), changes sign. This type of interface consists of a line of antiferromagnetic Ising bonds. Phase separation takes place at both sides of the preroughening transition for general values of $\langle h\rangle$.

The translation symmetry along the surface becomes spontaneously broken in the BCSOS flat and BCSOS rough phase. The Ising spins obtain long-range AF order. The heights on one sublattice become predominantly even and predominantly odd at the other. The ground state is twofold degenerate. The ensemble with fixed global height is grand canonical with respect to this type of order, but an interface can be imposed by means of boundary conditions (as discussed below). The order parameter ρ_s, see Eq. (2.6), changes sign across this type of

interface. It consists of a line of ferromagnetic Ising bonds, i.e., a line of missing bonds in the six-vertex lattice.

F. Interface free energies

We study the presence of long-range AF order in the DOF phase numerically from the finite-size-scaling behavior of these three types of interfaces. We determine the free energy in semi-infinite strips with periodic boundary conditions $h_{x,y}=h_{x+N_x,y}+a$, with $a=0,1,2$, and antiperiodic boundary conditions $h_{x,y}=-h_{x+N_x,y}+a$, with $a=0,1$ [where a is unique only mod(2)]. Define $\eta^{\pm}(a)$ as the difference in free energy between these boundary conditions and periodic boundary conditions with $a=0$. With the help of diagrams like the ones shown in Fig. 9, it is easy to show that these free energy differences are related to the Ising and six-vertex type interface free energies defined previously as

$$\begin{aligned}
&\eta^{+}(1)=\eta_s^{+}(1)+\eta_I^{\mathrm{F}}\pm\eta_I^{\mathrm{AF}}\ ,\\
&\eta^{+}(2)=\eta_s^{+}(2)+\eta_I^{\mathrm{F}}(2)\ ,\\
&\eta^{-}(0)=\eta_s^{-}(1)\ ,\\
&\eta^{-}(1)=\eta_s^{-}(0)+\eta_I^{\mathrm{F}}\pm\eta_I^{\mathrm{AF}}\ .
\end{aligned}\tag{2.9}$$

The $+$ ($-$) signs apply to even (odd) strip widths N. The various $\eta_s^{\pm}(a)$ reflect the different boundary conditions that can be imposed to a six-vertex model on a perfect square lattice (and therefore also on the random Ising-Bloch-wall lattice). η_I^{F} is the free energy of an Ising-Bloch wall, and η_I^{AF} the free energy of a line of ferromagnetic bonds in the AF ordered Ising phase. Notice that the (+,2) boundary condition imposes two Ising-Bloch walls into the systems, which unlike the conventional Ising model cannot annihilate each other since they carry parallel arrows.

The free energy of an Ising-Bloch-wall, η_I^{F}, is conjugate to ρ, and is nonzero only inside the RSOS flat phase. The free energy of a line of vacancies η_I^{AF} is conjugate to ρ_s, and is nonzero only inside the BCSOS flat and BCSOS rough phases. The free energies of the Néel-type interfaces $\eta_s^{+}(1)$ and $\eta_s^{-}(1)$ (the six-vertex-type degrees of freedom), are conjugate to ψ, and are nonzero only in the DOF and BCSOS flat phase.

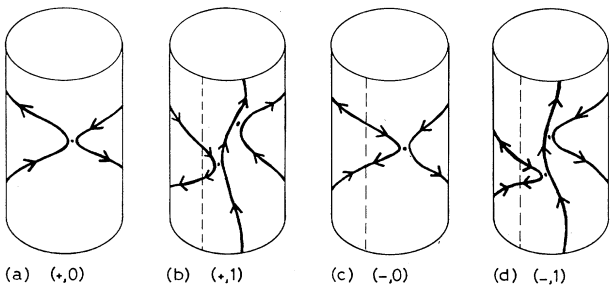

FIG. 9. Topological frustrations induced by the boundary conditions $h_{(x,y)}=\pm h_{(x+N,y)}+a$ for $(\pm,a)=(+,0)$, $(+,1)$, $(-,0)$, and $(-,1)$.

The step free energies scale as the inverse of the strip width N, with universal amplitudes, in the two rough phases. The six-vertex sector renormalizes into the Gaussian model according to the conventional KT renormalization arguments. This implies that the $\eta_s^{\pm}(a)$ scale as $\eta_s^{+}(a)=\frac{1}{2}K_g a^2 N^{-1}$ and $\eta_s^{-}(a)=\frac{1}{4}\pi N^{-1}$, with K_g^{-1} the roughness parameter defined in Eq. (2.2). The Bloch-wall free energy is equal to zero, $N\eta_I^{\mathrm{F}}=0$, in both rough phases, but the free energy of a line of vacancies is finite in the BCSOS rough phase, $\eta_I^{\mathrm{AF}}>0$, and zero in the RSOS rough phase.

K_g becomes equal to $\pi/2$ at the KT roughening transition line L-M-B. The separation, in Eq. (2.9), between Ising- and six-vertex-type degrees of freedom becomes meaningless along the other roughening transition line R-L, but the universal amplitudes take the same universal values: $\eta^{+}(a)=\frac{1}{2}K_g a^2 N^{-1}$ and $\eta^{-}(a)=\frac{1}{4}\pi N^{-1}$, with $K_g=\frac{1}{2}\pi$. Figure 10 shows the lines where $N\eta^{+}(2)=\pi$ for successive finite strip widths N between 2 and 8. These lines must converge in the thermodynamic limit to the roughening transition line (the line R-L-M-B in Fig. 2). In the Appendix we prove that $\eta^{+}(1)=\eta^{-}(1)$ along the line $\exp(-L_2)=2$ for all values of N. $\eta^{+}(1)=\frac{1}{2}K_g/N$ is smaller than $\eta^{-}(1)=\frac{1}{4}\pi N$ inside the rough phase, because $K_g<\frac{1}{2}\pi$. They become equal at the roughening transition (where $K_g=\frac{1}{2}\pi$). This implies that the two rough phases must terminate at the $\exp(L_2)\leq 2$ side of the phase diagram, or, most likely, that the roughening line L-M-B coincides with $\exp(L_2)=2$ (see the Appendix). Notice (see Fig. 10) that the finite size approximants for this segment of this roughening line are located at the "wrong" side $\exp(L_2)\geq 2$, but converge in a manner consistent with a location at $\exp(L_2)=2$.

The AF Ising transition line is the threshold where η_I^{AF} vanishes. We use the conventional analysis to determine the location of this line.[21] The sequence of lines where $N\eta_I^{\mathrm{AF}}$ for successive strip widths ($N=4,6,8,10$) cross must converge to the AF Ising critical line. We obtain η_I^{AF} from $\eta^{+}(1)-\frac{1}{4}\eta^{+}(2)$ inside the rough phase and from $\eta^{-}(1)$ on the flat side [see Eq. (2.9)]. We find that

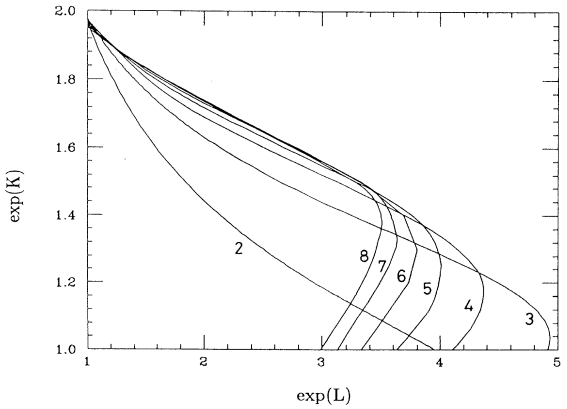

FIG. 10. Finite-size-scaling estimates of the KT roughening line, i.e., lines where $N\eta^{+}(2)=\pi$ for successive strip widths N from 2 to 8.

η_I^{AF} scales indeed as $N\eta_I^{AF}=2\pi x_H$ with the correct value of the magnetic critical exponent of the Ising model, $x_H=\frac{1}{8}$. For example, we find at point S in Fig. 2 $x_H=0.1245\pm0.001$,[18] and at point I (by extrapolation of the results in Fig. 11), $x_h=0.1245\pm0.001$. We also determine the value of the central charge c of conformal theory.[22] The free energy for periodic boundary conditions (PBC) must scale as $f_{PBC}\simeq f_{reg}+\frac{1}{6}c\pi N^{-2}$.[23] At point S we find $c=1.50\pm0.01$ in accordance with the above description of the transition as an Ising model ($c=\frac{1}{2}$) superimposed to a Gaussian model ($c=1$). Similarly, segment M-I represents a critical Ising model coupled to noncritical six-vertex degrees of freedom, i.e., $c=\frac{1}{2}$. Indeed we find $c=0.50\pm0.01$ at point I. Surprisingly, the Ising and six-vertex degrees of freedom do not seem to couple at the multicritical point M either (see Fig. 2). Preliminary results indicate that $c=1.5$ and no apparent singularities different from Ising.[24]

G. The preroughening transition

The most exciting aspect of the phase diagram is the presence of the preroughening transition line L-P. This is a new type of surface transition. The preroughening line is the threshold between the RSOS flat and DOF phase where η_I^F vanishes and $\eta_s^-(1)$ becomes nonzero. This implies [see Eq. (2.9)] that $\eta^-(1)$ vanishes [because $\eta_s^-(0)$ remains zero], and that $\eta^-(0)$ becomes finite. This is indeed what happens [see Figs. 11(d) and 11(c)]. This is conclusive evidence for the existence of the DOF phase and our interpretation of its character (positional disorder with long-range AF step order).

The central charge can be obtained again from the finite-size-scaling behavior of f_{PBC}. We find $c=1.00\pm0.01$ at point P. This suggests that the preroughening transition line is a critical line with continuously varying exponents. We determine the temperature critical exponent y_T at point P from the finite-size-scaling behavior of the temperature derivative of these quantities; we find $y_T=0.292\pm0.005$. So the specific-heat singularity is extremely weak,

$$\alpha=2-2/y_T=-4.85\pm0.1\ .$$

The numerical values for the universal finite-size-scaling amplitudes of the interface free energies at point P are

$$N\eta^+(1)=0.920\pm0.005\ ,$$

and

$$N\eta^+(2)=3.677\pm0.005\ .$$

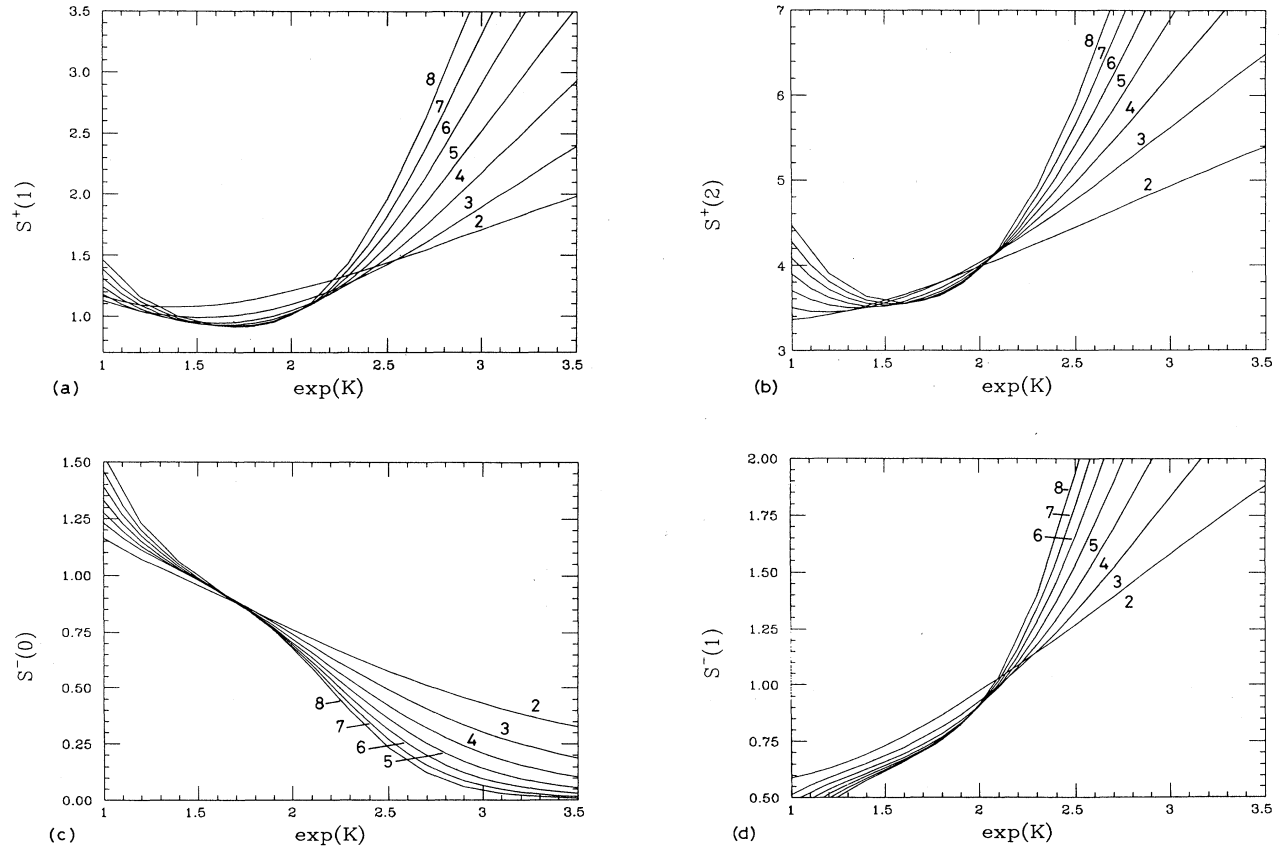

FIG. 11. Finite-size-scaling behavior of the surface tensions $\eta^{\pm}(a)=S^{\pm}(a)/N$ for strip widths $N=2,4,6,8,10$ along the line $L_2\to\infty$ in Fig. 2, for $(\pm,a)=(+,1)$, $(+,2)$, $(-,0)$, and $(-,1)$.

It is impossible to say with certainty from the present numerical data whether the critical exponents vary continuously along the preroughening line. The convergence becomes too slow close to the multicritical point L; slow convergence is consistent with the crossover to KT roughening. If indeed the exponents vary continuously, then y_T varies from $y_T=0$ at point L (its value at KT roughening, assuming continuity across point L) to $y_T=0.30$ at point P, and a similar continuous variation in the preceding universal amplitudes.

We have no exact analytical results yet about the scaling properties of the preroughening transition. However, the above numerical results give a hint. The structure of the phase diagram close to the multicritical point L somewhat resembles a so-called "critical fan," like the one in, e.g., the Ashkin-Teller model.[25] In that case the preroughening line would renormalize to the Gaussian model, with a continuously varying $K_g > \frac{1}{2}\pi$. In that case the universal amplitudes should still be Gaussian, i.e., $N\eta^+(a)=\frac{1}{2}a^2K_g$. This works. Our numerical values at point P obey

$$\eta^+(2)/\eta^+(1)=4.00\pm0.01 ,$$

with $K_g=1.54\pm0.01$. Moreover, the energy operator should remain the same as along the roughening line P-L, i.e., $\exp(i2\pi h_r)$. The $\exp(iqh_r)$ operators have critical exponents

$$x_q=2-y_q=q^2/(4\pi K_g)$$

in the Gaussian model.[16] This together with the earlier value of K_g predicts that

$$y_T=2-\pi/K_g=0.29\pm0.01 ,$$

which is consistent with our numerical result quoted above. Also our numerical values for the universal amplitudes of the antiperiodic boundary conditions,

$$N\eta^-(0)=0.785\pm0.005 ,$$

and

$$N\eta^-(1)=0.785\pm0.005$$

are consistent with the Gaussian value $N\eta^{\pm}(a)=\frac{1}{4}\pi$. So the operators along the preroughening line seem to obey the Gaussian-type operator algebra.

H. Suggestions for experiments

Preroughening and the DOF phase have not been studied experimentally yet. We close this section by pointing out several possible experimental ways to observe preroughening. One of the macroscopic manifestations of surface roughening is the vanishing of crystal facets with increasing temperature. The size of a facet is proportional to the step free energy $\eta^+(1)$. $\eta^+(1)$ vanishes at the roughening transition, and the crystal obtains a finite curvature. The jump in curvature is universal, proportional to the inverse of the roughness parameter K_g of Eq. (2.2).[26] Another macroscopic manifestation of surface roughening is the change in the growth rate as function of oversaturation. Below the roughening transition the crystal grows via nucleation of terraces. The growth rate depends exponentially on the oversaturation. The growth is linear in the rough phase. The rate becomes proportional to the oversaturation, because the particles can adhere at the steps (see, e.g., Gallet *et al.*[14]).

Studies of these two macroscopic effects for ^{4}He crystals in coexistence with their superfluid[14] are among the most detailed experimental confirmations of the KT nature of the surface roughening transition. In the presence of a DOF phase these two effects must take place at different temperatures. The growth changes from nucleation to linear growth at the preroughening transition, while the crystal facet does not disappear until the roughening transition (with the same universal jump in the curvature as before).

Surface roughening has also been studied in detail for metal surfaces, in particular for vicinal surfaces of Ni and Cu.[15] In the rough phase the line shapes are power laws. They are determined by the correlation functions

$$G_q(r)=\langle \exp\{iq[h(r_0+r)-h(r_0)]\}\rangle \sim r^{-2x_q} , \qquad (2.10a)$$

with $x_q=q^2/(4\pi K_g)$. Using this, the roughness parameter K_g has been extracted from line shapes in atomic beam experiments for Ni($11m$) surfaces.[15] These experiments confirm the KT nature of the roughening transition; at the temperature where the power law ceases to be a good fit to the line shape the roughness parameter takes the predicted universal value, $K_g=\pi/2$.

The DOF phase can be observed from the line shape in this type of atomic beam and x-ray experiments as follows. The Ising-type correlation function Eq. (2.4), which couples to the parity, corresponds to the correlation function in Eq. (2.10a) at the anti-Bragg angle $q=\pi$. So $G_\pi(r)$ decays exponentially to a constant in the flat crystal phase,

$$G_\pi(r)\sim \exp\left[-a\frac{r}{\xi}\right]+\rho^2 , \qquad (2.10b)$$

but exponentially to zero in the DOF phase

$$G_\pi(r)\sim \exp\left[-a\frac{r}{\xi}\right] . \qquad (2.10c)$$

$G_\pi(r)$ decays as a power law at the preroughening temperature,

$$G_\pi(r)\sim r^{-2x_\pi} , \qquad (2.10d)$$

and the parity order parameter ρ of Eq. (2.5) vanishes as

$$\rho\sim(T-T_{PR})^{\beta} . \qquad (2.11)$$

Assume that along the preroughening line the aforementioned Gaussian operator algebra applies, i.e., that

$$x_q=2-y_q=q^2/(4\pi K_g)$$

and $y_T=2-x_{2\pi}$. Then $\beta=(2-y_\pi)/y_T$ varies continu-

ously along the preroughening line between the values $\beta=1.46\pm0.06$ at point P in Fig. 2 (where $K_g=1.84\pm0.01$) and $\beta=\infty$ at the multicritical point L. The preroughening transition is followed at higher temperatures by a conventional roughening transition. There the line-shape changes into the power law Eq. (2.10a), with the usual universal value $K_g=\frac{1}{2}\pi$ at T_R.

It is difficult to predict which experimental systems exhibit preroughening. The multicritical point L, where the DOF phase becomes stable, is located in Fig. 2 at $L_2/K=1.23\pm0.04$. In general one might expect that the interactions of an experimental system can be cast approximately into a Hamiltonian of the form

$$H=\sum_{\langle r,r'\rangle} V(|r-r'|)[h(r)-h(r')]^2 . \tag{2.12}$$

K and L_2 in Eq. (2.1) are related to $V(r)$ as $K=V(1)$ and $L_2=4V(\sqrt{2})$. L_1 is equal to zero in Fig. 2, but equal to $L_1=\frac{1}{4}L_2=V(\sqrt{2})$ in Eq. (2.12). L_1 renormalizes the step energy K; roughly as $K_{\rm eff}\simeq K+2L_1$. So in systems like Eq. (2.12) a DOF phase can be expected if $L_2/K_{\rm eff}\simeq1.23$, i.e., if $V(\sqrt{2})/V(1)\simeq0.8$. In other words, we expect the onset of a DOF phase if the combined strength of all the further than nearest-neighbor interactions (within the interaction range) is approximately equal to the nearest-neighbor strength. It is not clear to us whether this is satisfied in ^{4}He. It might be satisfied in metals, because the observation of nonzero roughening temperatures in higher-order vicinal metal surfaces, like Ni(11m) and Cu(11m), for $m=3,5,7,\ldots$,[15] implies that the steps interact over large distances.

III. EQUIVALENCE BETWEEN SOS MODELS AND SPIN QUANTUM CHAINS

A. Transfer matrix of the RSOS model

In this section we derive in detail the equivalence between the RSOS model and the spin-1 chain using the transfer matrix formalism. We choose the transfer matrix of the RSOS model in the diagonal direction as indicated in Fig. 12 by the dashed lines. The column heights h_n' represent the heights h_n one unit of "time" later. The transfer matrix has the form

$$T=\left[\prod_{n\ \rm even} T_t(n)T_K(n)T_l(n)\right]\left[\prod_{n\ \rm odd} T_t(n)T_K(n)T_L(n)\right] , \tag{3.1}$$

with

$$\begin{aligned}
T_K(n)&=\exp\{-K[\delta(|h_{n+1}-h_n|-1)\\
&\quad+\delta(|h_{n-1}-h_n|-1)]\} ,\\
T_L(n)&=\exp[-L_1^{(x)}\delta(|h_{n+1}-h_{n-1}|-1)\\
&\quad-L_2^{(x)}\delta(|h_{n+1}-h_{n-1}|-2)] ,\\
T_t(n)&=P(h_{n+1},h_n)P(h_n,h_{n-1})\\
&\quad\times\{1+2\tau_1[1+q\delta(|h_{n+1}-h_{n-1}|-1)]\\
&\quad\times\cos(p_n)+2\tau_2\cos(2p_n)\} ,
\end{aligned} \tag{3.2}$$

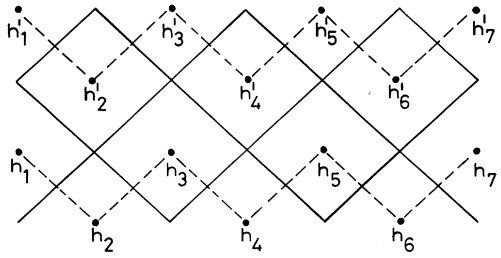

FIG. 12. Diagonal lattice setup used in the transfer matrix. The dashed lines connect column height variables that belong to the same time slice.

where

$$\begin{aligned}
\tau_1&=\exp(-L_1^{(t)}) ,\\
\tau_2&=\exp(-L_2^{(t)}) ,\\
q&=\exp(-Q)-1 .
\end{aligned} \tag{3.3}$$

The operators h_n and p_n obey the conventional scalar commutation relation $[h_n,p_m]=i\delta_{n,m}$, but with as a constraint that the eigenvalues of h_n are integers, and accordingly the spectrum of p_n is periodic, $0<p_n\le2\pi$. The $P(k,l)$ are projection operators that enforce the step-one constraint: $P(k,l)=1$ if $|k-l|\le1$ and $P(k,l)=0$ otherwise.

Next, introduce the spin-1 algebra,

$$\begin{aligned}
S_n^z&=h_{n+1}-h_n ,\\
S_n^{\pm}S_{n-1}^{\mp}&=2P(h_{n+1},h_n)P(h_n,h_{n-1})e^{\pm ip_n} ,
\end{aligned} \tag{3.4}$$

with $S_n^x=\frac{1}{2}(S_n^++S_n^-)$, $S_n^y=(1/2i)(S_n^+-S_n^-)$, and $[S_n^x,S_m^y]=iS_n^z\delta_{m,n}$. $S_n^z=0$ represents the absence and $S_n^z=+1$ (-1) the presence of an up (down) step, at the bond between sites n and $n+1$ in Fig. 12. In terms of the spin-1 operators the transfer matrix reads

$$\begin{aligned}
T_K(n)&=\exp\{-K[(S_{n-1}^z)^2+(S_n^z)^2]\} ,\\
T_L(n)&=\exp\{-L_1^{(x)}[(S_{n-1}^z)^2+(S_n^z)^2]-\tfrac{1}{2}L_2^{(x)}S_n^zS_{n-1}^z\\
&\quad+(2L_1^{(x)}-\tfrac{1}{2}L_2^{(x)})(S_n^zS_{n-1}^z)^2\} ,\\
T_t(n)&=\{1+\tfrac{1}{2}\tau_1[1+q\delta(|S_n^z+S_{n-1}^z|-1)]\\
&\quad\times(S_n^+S_{n-1}^-+S_n^-S_{n-1}^+)\\
&\quad+\tfrac{1}{4}\tau_2[(S_n^+S_{n-1}^-)^2+(S_n^-S_{n-1}^+)^2]\} .
\end{aligned} \tag{3.5}$$

B. The spin-1 quantum Hamiltonian

The logarithm of the transfer matrix $H=-\ln(T)$, defines the one-dimensional quantum problem associated with the RSOS model. The ground-state energy of H is proportional to the free energy. The quantum fluctuations play the role of the thermodynamic fluctuations. The reduced Hamiltonian H_R is obtained by ignoring that the factors in the right-hand side in Eq. (3.1) do not commute,

$$H_R=\sum_n \{-\tfrac{1}{2}\tau_3(S_n^+S_{n-1}^- + S_n^-S_{n-1}^+) - \tfrac{1}{4}\tau_2[(S_n^+S_{n-1}^-)^2+(S_n^-S_{n-1}^+)^2]$$
$$-\tfrac{1}{2}(\tau_3-\tau_1)[S_n^zS_{n-1}^z(S_n^+S_{n-1}^- + S_n^-S_{n-1}^+)+(S_n^+S_{n-1}^- + S_n^-S_{n-1}^+)S_n^zS_{n-1}^z]$$
$$+D(S_n^z)^2+JS_n^zS_{n-1}^z+\Delta(S_n^zS_{n-1}^z)^2\}\ , \tag{3.6}$$

with

$$\tau_3=(1+q)\tau_1\ ,$$
$$D=2(K+L_1^{(x)})\ ,$$
$$J=\tfrac{1}{2}L_2^{(x)}\ ,$$
$$\Delta=-(2L_1^{(x)}-\tfrac{1}{2}L_2^{(x)})\ . \tag{3.7}$$

H_R becomes exactly equal to $H=-\ln(T)$ in the so-called time continuum limit where K, $L_1^{(x)}$, $L_2^{(x)}$, τ_1, τ_2, and τ_3 go to zero simultaneously with fixed ratios. This corresponds to the limit where the 2D lattice becomes very anisotropic; $L_1^{(t)}$ and $L_2^{(t)}$ go to infinity. In most statistical-mechanics models the universality class of the phase transitions and the general structure of the phase diagram do not change in this limit (see, e.g., Refs. 16 and 26). Lattice anisotropy is associated with the stress tensor, and this is a redundant operator for most phase transitions. This aspect plays an important role also in the recent applications of conformal theory to 2D critical phenomena.[22]

However, there are exceptions. The structure of the phase diagram changes quite dramatically in cases where the ground state modulates in the timelike direction. This is the reason why we choose the diagonal direction setup of the transfer matrix; it allows us to consider the BCSOS-type ground state at negative values of K. In our setup the topology of the phase diagrams of the spin-1 Hamiltonian Eq. (3.6) (the very anisotropic RSOS model) and the isotropic RSOS model, Eq. (2.1), are the same as long as the next-nearest-neighbor interactions are ferromagnetic in the timelike direction, $0<\tau_1\le 1$ and $0<\tau_2\le 1$.

Equation (3.6) is the most general spin-1 Hamiltonian, with only nearest-neighbor interactions between the spins, which conserves the total spin and is invariant under spin reversal. It is the unique reduced Hamiltonian of the transfer matrix of the RSOS model Eq. (2.1). The reverse is not true. There are many ways to discretize time in the Feynman path integral. The spin-1 Hamiltonian Eq. (3.6) is equivalent to many (slightly different) RSOS models. Indeed, the interactions in our RSOS model, Eq. (2.1), are somewhat different from the ones obtained in earlier work where time was discretized in the spin-1 model by means of the Trotter formula.[27]

In Sec. II we found that the phase diagram of the RSOS model becomes completely transparent if we interpret the RSOS model as an annealed bond-diluted six-vertex model. Similarly, in the next section we will find that the phase diagram of the quantum chains become much more transparent if we interpret Eq. (3.6) as the Hamiltonian of a diluted spin-$\frac{1}{2}$ chain instead of a chain of spin-1 objects. Let $S_n^z=0$ represent the state where site n is empty, and $S_n^z=+1,-1$ the state where site n is occupied by a spin-$\frac{1}{2}$ particle with, respectively, spin-up or spin-down. The steps in the crystal surface configurations represent the world lines of these spin-$\frac{1}{2}$ particles. The vertical direction in Fig. 3 and Fig. 9 now plays the role of (imaginary) time.

C. SOS models in general

The derivation presented here can be generalized to SOS models in general. SOS models where the step heights are less restricted, e.g., to

$$\delta h=0,\pm1,\pm2,\ldots,\pm s\ ,$$

are equivalent to quantum chains with larger integer spin s. They can be interpreted as describing diluted spin-$(s-\frac{1}{2})$ chains with analogous dynamics as in Eq. (3.6). Again the steps in the surface play the role of the world lines of these particles.

Quantum chains with half-integer spins are equivalent to body-centered solid-on-solid (BCSOS) models. BCSOS models describe surfaces with body-centered type of symmetry such as Ni(110) and Cu(110). We refer to the literature for the well-known equivalence, using the same procedure as described here, between the BCSOS model (the six-vertex model) and the spin-$\frac{1}{2}$ quantum chain[17,28] [or simply set $K\to-\infty$ in Eqs. (2.1) and (3.7)]. The generalization to half-integer spin chains with larger spin is straightforward.

IV. THE PHASE DIAGRAM OF THE SPIN-1 QUANTUM CHAIN

A. Diluted spin-$\frac{1}{2}$ representation

In this section we explain the phase diagram of the spin-1 chain. The structure becomes quite transparent if we interpret the spin-1 chain as a gas of spin-$\frac{1}{2}$ particles. The world lines of these particles are the direct analogues of the steps in the 2D crystal surface in the statistical-mechanical RSOS model representation. The Heisenberg antiferromagnetic (HAF) point lies inside the DOF phase. This clarifies the so-called Haldane conjecture. Moreover, in Secs. V and VI we show that valence bond solid (VBS) type phases in quantum spin chains are equivalent to disordered flat (DOF) phases. This identification with the DOF phase implies that at the HAF point and the VBS phase the spins have long-range order. The spin-$\frac{1}{2}$ particles are in a fluid (positional disordered) state but maintain long-range AF spin order. Néel solitons have finite mass. Using the results of Sec. II, we identify order parameters that distinguish the VBS phase from the other phases. This interpretation of the model as a diluted spin-$\frac{1}{2}$ chain explains the physical

mechanism responsible for the stability of the VBS phase.

Equation (3.6) is the most general spin-1 quantum chain Hamiltonian with only nearest-neighbor interactions and dynamics that conserve the total z component of the spin. Likewise, Eq. (2.1) is the most general RSOS model where steps only interact when they meet at the vertex sites **R** (see Fig. 1). The phase diagram of the RSOS model is six dimensional because Eq. (2.1) contains six coupling constants. The phase diagram of the spin-1 chain, Eq. (3.6), is five dimensional. It is contained in the RSOS model as the limit where the lattice becomes extremely anisotropic (see Sec. III B). Or alternatively, the RSOS model can be viewed as a discretized time generalization of the spin-1 quantum chain; the extra sixth coupling constant represents the timelike lattice constant.

In Sec. II we found that the phase diagram of the RSOS model becomes completely transparent if we interpret the RSOS model as an annealed bond-diluted six-vertex model, i.e., a six-vertex model defined on an ensemble of lattices formed by the Bloch walls of an Ising model. The coupling constants K, $L_1^{(x)}$, $L_1^{(t)}$, and Q in Eq. (2.1) govern the Ising-type order, i.e., the average structure of the annealed six-vertex model lattice, whereas $L_2^{(x)}$ and $L_2^{(t)}$ govern the six-vertex-type order.

To reformulate this into spin-1 language we interpret the spin-1 model as a one-dimensional gas of spin-$\frac{1}{2}$ particles. $S_n^z=0$ represents the state where site n is empty, and $S_n^z=+1,-1$ the state where site n is occupied by a spin-$\frac{1}{2}$ particle with, respectively, spin-up or spin-down.

The step excitations on the crystal surface represent the world lines of these spin-$\frac{1}{2}$ particles. The vertical direction in Fig. 3 and Fig. 9 now plays the role of (imaginary) time. The Ising-Bloch walls represent the presence of spin-$\frac{1}{2}$ particles and the arrows of the six-vertex model represent their spin.

From this perspective Eq. (3.6) is indeed the most general Hamiltonian with nearest-neighbor interactions. There are only four characteristic configurations for nearest-neighbor sites: $(S_n^z,S_{n-1}^z)=(0,0)$, $(+,0)$, $(+,+)$, or $(+,-)$. Hence we need three terms in H that commute with S_n^z: D to represent the chemical potential of the spin-$\frac{1}{2}$ particles, J to represent the interactions between the spins of the particles, and Δ to represent a soft-core repulsion between the particles at nearest-neighbor sites. Furthermore, there are only three characteristic dynamical processes: a particle pair with opposite spin can be created or annihilated at nearest-neighbor sites with probability τ_1, e.g., $(0,0)\rightarrow(+,-)$, a particle pair at nearest-neighbor sites can exchange their spins with probability τ_2, e.g., $(+,-)\rightarrow(-,+)$, a particle can hop to a nearest-neighbor site with probability τ_3, e.g., $(0,+)\rightarrow(+,0)$.

B. Phase diagram of the spin-1 chain

Figure 2 shows the phase diagram of the RSOS model in the subspace where the lattice is isotropic, $L_2=L_2^{(x)}=L_2^{(t)}$ and $L_1=L_1^{(x)}=L_1^{(t)}$, and steps with parallel arrows repel each other, $L_2>0$, while steps with antiparallel arrows do not attract each other, $L_1=Q=0$ (see Sec. II B). During the last 5 years there have been many numerical studies of the spin-1 quantum chain. Most have focused on the special case where $\tau_2=\Delta=\tau_3-\tau_1=0$.[2] These results lead to the schematic phase diagram shown in Fig. 13. In Fig. 13(a) we label all the phases according to the RSOS model representation (compare with Fig. 2), in Fig. 13(b) according to the conventional spin-1 nomenclature, and in Fig. 13(c) according to the interpretation of the spin-1 model as a gas of spin-$\frac{1}{2}$ particles. For the first time we obtain a comprehensive understanding of this phase diagram. Moreover, some aspects had been unclear up to now. In particular, the existence of the transition line L-N had been acknowledged only recently,[27,2] but its nature (it is the preroughening transition) and the distinction between the two singlet phases, the RSOS flat phase and the DOF phase, remained obscure. Another important detail is the exact location of the "roughening" transition line L-M-B. We will show that it exactly coincides with the D axis. Previous numerical studies placed it at the $J>0$ side.

In Sec. II we mentioned that it is useful to view the phase diagram as a superposition of the familiar phase diagrams of the Ising model and the six-vertex model. All differences in structure between Figs. 2 and 13 can be completely understood from this. For example, the absence of the multicritical point N and a first-order transition line between the RSOS and BCSOS flat phases beyond N, in Fig. 2 reflects the absence of next-nearest-neighbor interactions L_1 and four-spin interactions Q in the Ising sector.

In Sec. II we discussed the structure of the phase diagram from the surface roughening perspective. For clarity we now repeat this discussion using the diluted spin-$\frac{1}{2}$ chain interpretation.

The density of spin-$\frac{1}{2}$ particles is controlled in Figs. 2 and 13 by the coupling constant along the vertical axes, K and D, respectively, while the order of their spins is controlled by the coupling constant along the horizontal axis, L_2 and J, respectively.

In the limit $D\rightarrow-\infty$ each site is occupied, and the spin-1 quantum Hamiltonian, Eq. (3.6), reduces to the exactly soluble spin-$\frac{1}{2}$ quantum chain (the six-vertex model).[8] The particles form a solid.

The BCSOS flat phase at $J\gg0$ and $D\ll0$ (the Néel phase), represents a solid of spin-$\frac{1}{2}$ particles with long-range spatial order and also long-range AF spin order. At finite values of D not every site is occupied (there are holes), but until the Ising transition line, the particles maintain their positional solid-type order. It is a solid with virtual excitations of bound hole pairs (the Ising dynamics allows particles to be annihilated or created at nearest-neighbor sites only in pairs).

The BCSOS rough phase at $J\simeq0$ and $D\ll0$, represents a solid of spin-$\frac{1}{2}$ particles, with long-range positional order, but massless spin-wave excitations. The spin exchange J between the particles at nearest-neighbor sites is too weak to stabilize AF or F long-range spin order.

The BCSOS stepped phase, at $J\ll0$, represents a solid

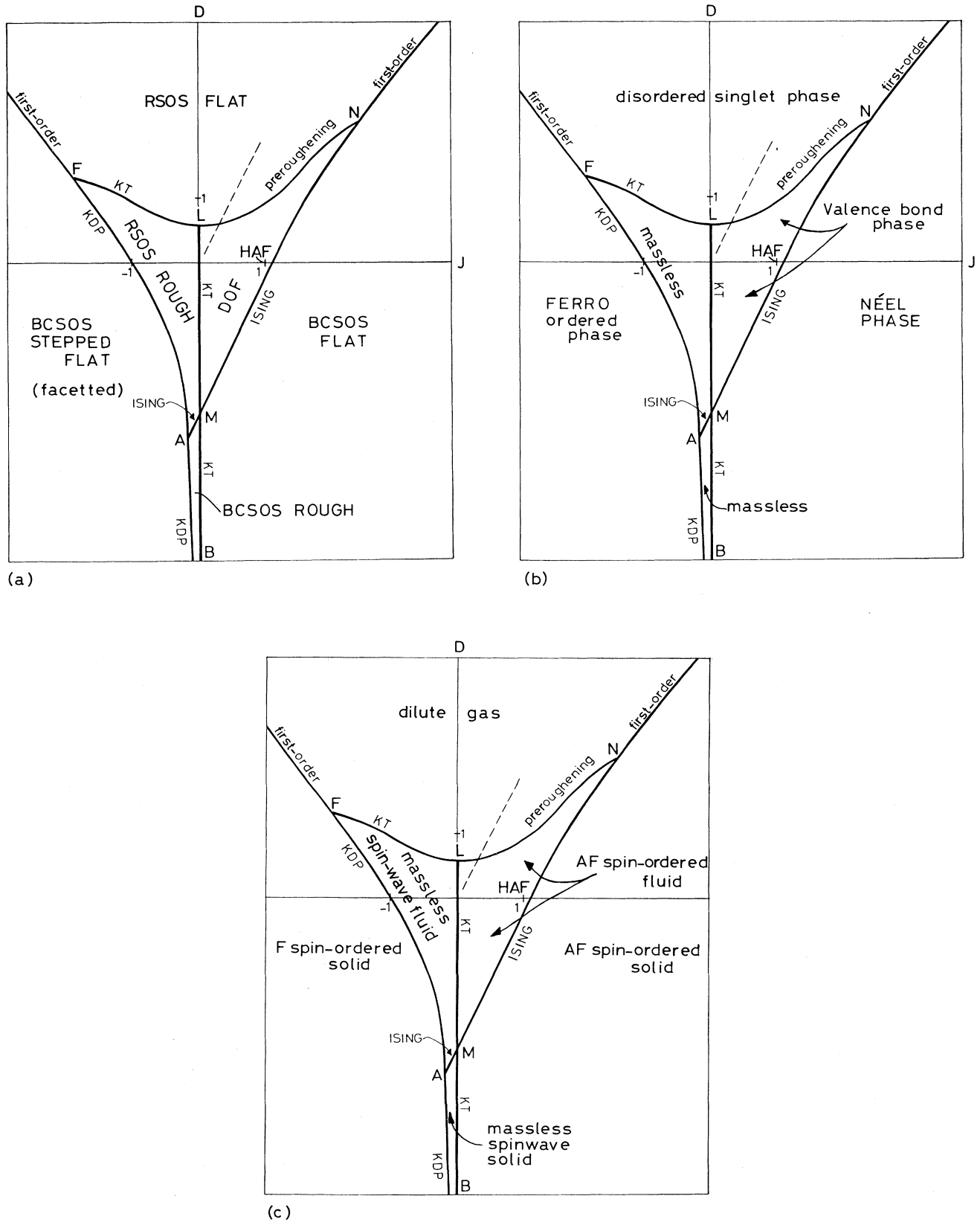

FIG. 13. Phase diagram of the spin-1 Hamiltonian with particle fugacity D and AF spin interaction J, with $\tau_3=1$, using the RSOS model language (a), the spin-1 nomenclature (b), and the interpretation of the spin-1 chain as a diluted spin-$\frac{1}{2}$ chain (c).

of spin-$\frac{1}{2}$ particles with perfect ferromagnetic spin order. This phase is perfectly ordered because the ferromagnetic ground state is frozen with respect to each of the three types of dynamical processes.

The hole-pairs unbind at the Ising transition line N-M-A. The solid melts into a fluid, a dense state without positional order. The RSOS rough phase, at $J \simeq 0$ and $D \simeq 0$, represents a fluid of particles with massless spin-wave excitations. The disordered flat (DOF) phase, at $J \gg 0$ and $D \simeq 0$, which we will identify in Sec. V with the VBS phase, represents a fluid of spin-$\frac{1}{2}$ particles, with long-range AF spin order.

This fluid collapses at the KT line F-L and the preroughening transition line L-N. The RSOS flat phase, at $D \gg 0$, represents a gas with only virtual excitations of bound pairs of spin-$\frac{1}{2}$ particles with opposite spin. (They are the terraces in the crystal surface.) This gas is too dilute to be able to sustain long-range spin order, or massless spin waves.

The line L-M-B is a Kosterlitz-Thouless (KT) transition line, in accordance with our separation of positional (Ising) and spin-$\frac{1}{2}$ (six-vertex) types of degrees of freedom. In the RSOS model interpretation this is simply the roughening transition. From the spin-1 chain perspective this transition is driven by the "umklapp excitations" in the spin-$\frac{1}{2}$ sector.[29]

The line F-A-B, where the spin-$\frac{1}{2}$ particles freeze into the perfectly F ordered state, is a KDP type first-order transition.[30,8]

The gas phase (RSOS flat phase) contains bound pairs of spin-$\frac{1}{2}$ particles with opposite spin. These bound pairs unbind along its phase boundary. To the left of point F and to the right of point N this is a simple first-order transition. Along the F-L segment this is the conventional Kosterlitz-Thouless type roughening transition, in accordance with conventional renormalization arguments for the RSOS model[11] (i.e., the continuum limit which maps the spin-1 quantum chain into the quantum sine-Gordon model[31]). The line L-N is the novel preroughening transition. In Sec. II we discussed its scaling properties, and found that it almost certainly is a line with continuously varying critical exponents (with central charge $c=1$). The particles unbind into a random (fluid) type structure, but maintain long-range AF spin order. At first sight this transition resembles a conventional Ising transition, but the extra spin degrees of freedom carried by the Ising-Bloch walls weaken the transition considerably (see Sec. II G).

C. Order parameters

It is important to translate the order parameters which we defined in Sec. II to distinguish between the DOF phase and the RSOS flat phase into the spin-1 language. Both are so-called singlet phases, where

$$m = \langle 0 | S_n^z | 0 \rangle = 0 \ . \tag{4.1}$$

This simply states that both describe flat crystal surfaces. The translation symmetry in the vertical-z direction, $h \rightarrow h+1$, is spontaneously broken in both phases, with an average integer height h in the RSOS flat phase and average half-integer height h in the DOF phase.

It is impossible to define local order parameters that distinguish these two phases. The local order parameters of Sec. II E become nonlocal string operators in the spin-1 formulation (where the surface configuration is characterized by the steps). Recall the Ising-type order parameter ρ, Eq. (2.5), which is finite in the RSOS flat phase and zero everywhere else. The limiting value of the parity correlation function, Eq. (2.4),

$$G_H(n) = \left\langle 0 \left| \exp\left[i\pi \sum_{m=n_0}^{n+n_0} S_m^z \right] \right| 0 \right\rangle , \tag{4.2}$$

is equal to ρ^2. So we can determine the absolute value of ρ, i.e., the presence of Ising spin order, but we cannot determine the sign of ρ (distinguish between the two ferromagnetic Ising ground states). ρ can be written as

$$\rho = \left\langle 0 \left| \exp(i\pi h_0) \exp\left[i\pi \sum_{m=1}^{n} S_M^z \right] \right| 0 \right\rangle , \tag{4.3}$$

with h_0 the height of the column at the seam between spins S_N^z and S_1^z. It is necessary to enlarge the Hilbert space with this variable, h_0. It ensures that the mapping from column height configurations to spin configurations is one to one. h_0 changes by one when a particle passes by or a particle pair is being created or annihilated at the seam; e.g., h_0 changes into h_0+1 when a spin-$\frac{1}{2}$ particle with down spin moves from site N to 1. The information about the absolute height of the surface is lost in the spin representation in the absence of h_0, and the sign of ρ becomes meaningless (see also Sec. VI A).

Similarly, the order parameter ψ, Eq. (2.8), which vanishes everywhere except in the DOF and BCSOS flat phase becomes

$$\psi = \left\langle 0 \left| \exp(i\pi h_0) \exp\left[i\pi \sum_{m=1}^{n} S_M^z \right] S_n^z \right| 0 \right\rangle , \tag{4.4}$$

and its square is the limiting value of the correlation function, Eq. (2.7),

$$G_s(n) = \left\langle 0 \left| S_{n_0}^z \exp\left[i\pi \sum_{m=n_0}^{n+n_0} S_m^z \right] S_{n+n_0}^z \right| 0 \right\rangle . \tag{4.5}$$

Finally, the order parameter ρ_s, Eq. (2.6), which vanishes everywhere except inside the BCSOS flat phase, also becomes nonlocal,

$$\rho_s = \left\langle 0 \left| \exp(i\pi h_0)(-1)^n \exp\left[i\pi \sum_{m=1}^{n} S_M^z \right] \right| 0 \right\rangle . \tag{4.6}$$

The translation symmetry is broken in the direction along the surface in the BCSOS flat phase. Therefore we can use the staggered magnetization as a local parameter:

$$m_s = \langle 0 | (-1)^n S_n^z | 0 \rangle \ . \tag{4.7}$$

The order parameter ρ_s couples only to the positional order and ψ only to the spin-$\frac{1}{2}$ order, but m_s couples to

both: $m_s \simeq \rho_s \psi$. For example, the AF spin order becomes perfect in the limit $J \to \infty$, $\psi = \pm 1$. There, $|m_s|$ is equal to $|\rho_s|$, and decreases for increasing D until it vanishes at the AF Ising transition point I, while the order parameter ψ remains nonzero inside the DOF phase. Similarly, the particle order becomes perfect (the solid) in the limit $D \to -\infty$, $\rho_s = \pm 1$. There, $|m_s|$ is equal to $|\psi|$, and decreases for decreasing J until it vanishes at the KT transition line at $J=0$, while ρ_s remains nonzero inside the BCSOS rough phase.

D. Mass gaps

We do not calculate these correlation functions numerically.[32] Instead we focus on the mass gaps conjugate to these order parameters, the mass of the spin-$\frac{1}{2}$ particles and Néel solitons. These are the interface free energies of Sec. II F. We study the finite-size-scaling properties of the ground-state energies of chains with lengths $N=2,4,\ldots,12$, for periodic boundary conditions $S^z_{n+N} = +S^z_n$ with total magnetization $\sum_n S^z_n = 0,1,2$, and for antiperiodic boundary conditions $S^z_{n+N} = -S^z_n$ with total magnetization $\sum_n S^z_n = 0,1$ [mod(2)]. The mass gaps are the differences in these ground-state energies

$$\eta^{\pm}(a) = E_0^{\pm}(a) - E_0^{+}(0) \ .$$

Figure 9 shows the world lines of the topologically induced frustrations and Eq. (2.9) gives the separation between positional and spin type masses.

The Ising-type surface tension η_I^{F}, see Eq. (2.9), represents the mass of the spin-$\frac{1}{2}$ particles in the gas phase (the RSOS flat phase), and is conjugate to the order parameter ρ. It vanishes at the transition line F-R-L-P-N, and is zero everywhere else.

The surface tension η_I^{AF} represents the mass of a hole inside the two solid phases (the BCSOS flat and BCSOS rough phase), and is conjugate to the order parameter ρ_s. It vanishes at the Ising transition line A-S-M-I-N, and is zero everywhere else.

The surface tensions $\eta_s^{\pm}$ represent the mass of a Néel soliton inside the AF spin ordered fluid and solid phase (the DOF and BCSOS flat phase), and are conjugate to the order parameter ψ. They vanish along the preroughening line L-P-N, and roughening line L-M-B, and are zero everywhere else.

In Sec. II we describe in detail how we use these properties to determine the phase boundaries in Fig. 2. We do not repeat this calculation for Fig. 13, because most phase boundaries have been studied extensively by many earlier numerical studies of the spin-1 chain.[2] The only exception is the preroughening transition and the nature of the DOF phase.

In Sec. II we present numerical evidence for the existence of the DOF phase and the validity of our interpretation of it by calculating the finite-size-scaling behavior of $\eta^-(1)$ and $\eta^-(0)$ across the preroughening line. See Eq. (2.9): $\eta^-(0) = \eta_s^-(1)$, which represents the Néel soliton mass, must be zero inside the gas phase (RSOS flat phase) and be nonzero inside the AF ordered fluid (DOF phase). $\eta^-(1) = \eta_I^{\mathrm{F}} + \eta_s^-(0)$, which represents the particle mass, must be zero inside the AF ordered fluid (DOF flat phase) and be nonzero inside the gas phase (DOF phase). This is indeed what happens. Figure 11 shows the scaling behavior across the preroughening transition in the isotropic RSOS model of Fig. 2 in the limit $L_2 \to \infty$. As predicted, $N\eta^-(1)$ shown in Fig. 11(d) diverges in the RSOS flat phase and vanishes in the DOF phase, while $N\eta^-(0)$ shown in Fig. 11(c), vanishes in the RSOS flat phase and diverges in the DOF phase.

Figure 14 shows how the same quantities behave in the spin-1 chain along the dashed line in the phase diagram Fig. 13. The results converge less rapidly, because of the nearness of the KT and AF Ising transition lines. In the RSOS model we decided to study a cut through the six-dimensional phase diagram, where the multicritical point N has moved to infinity, to minimize this type of interference. However, the results support that the spin-wave mass gap, $\eta_s^-(1)$, is nonzero in the VBS phase and zero inside the disordered singlet phase, and that the particle mass, η_I^{F}, is zero inside the VBS phase and nonzero inside the disordered singlet phase.

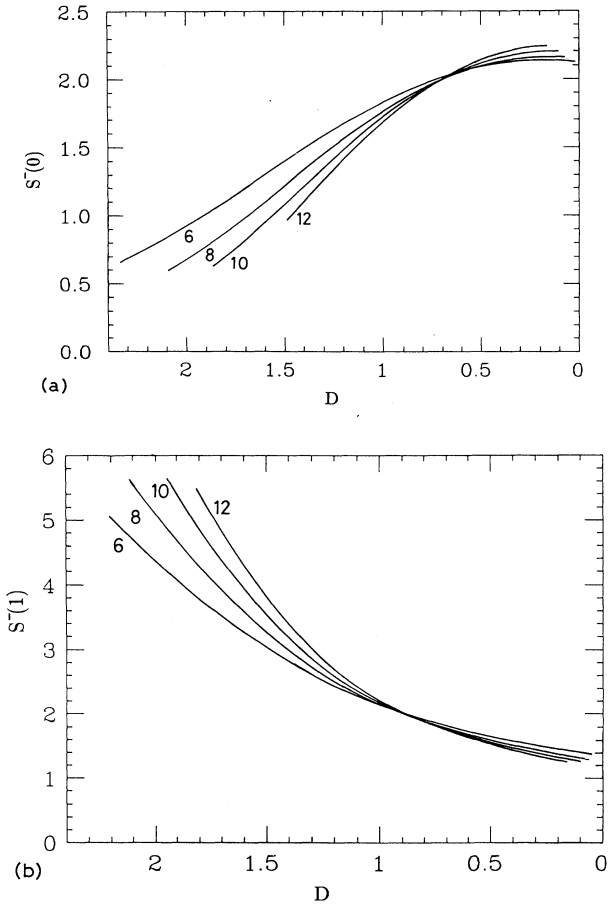

FIG. 14. Finite-size-scaling behavior of the surface tensions $\eta^-(0) = S^-(0)/N$, and $\eta^-(1) = S^-(1)/N$, along the dashed line in Fig. 13, for strip widths $N=4,6,8,10,12$.

E. Exact location of the KT transition

Most of the recent interest in the ground-state properties of the spin-1 quantum chain has been triggered by the Haldane conjecture,[1] which states that the energy spectrum at the Heisenberg AF (HAF) point is not massless, but that there is an energy gap between the ground state and the first excited state. At first this conjecture was controversial, but more recent numerical studies have demonstrated quite convincingly the presence of a finite mass gap at this point.[2] The point $(J,D)=(1,0)$ in Fig. 13 corresponds to the HAF point. This point clearly lies inside the DOF phase.

We will now remove any remaining doubt that the HAF point might belong to the massless rough phase, by showing that the roughening line L-M-B must be located to the left or (most likely) exactly at the D axis. In the Appendix we prove that $\eta^+(1)=\eta^-(1)$ in the subspace

$$\exp(-L_2^{(x)})+\exp(-L_2^{(t)})=1 ,$$

for all values of the strip width N. It must be true that inside the rough phase $N\eta^+(1)=\nu K_g/2$, with $K_g<\pi/2$, and $N\eta^-(1)=\nu\pi/4$. With ν a common scale factor (proportional to the spin-wave velocity) which is equal to $\nu=1$ in the isotropic lattice. So $\eta^+(1)$ and $\eta-(1)$ cannot be equal inside the rough phase; except at the roughening transition itself where $K_g=\pi/2$. This implies in Fig. 2 that the roughening line L-M-B must be located at $\exp(L_2)\leq 2$ and most likely exactly at $\exp(L_2)=2$ (see the Appendix). It implies that in Fig. 13 the KT-transition line L-M-B must be located at the $J<0$ side of the phase diagram, and most likely that it coincides with the D axis. Recall that

$$\tau_2=\exp(-L_2^{(t)})=0$$

and $J=\frac{1}{2}L_2^{(x)}$; hence $\exp(-L_2^{(x)})=1$ corresponds to $J=0$. Most numerical studies place this transition line at the $J>0$ side (the wrong side),[2,27] but this is consistent with our own numerical work for the RSOS model, Fig. 10, and slow numerical convergence.

The value of ν is unknown because the spin-1 chain corresponds to a RSOS model on an extremely anisotropic lattice ($\nu=1$ on an isotropic lattice). Therefore the condition $N\eta^+(2)=\pi$ cannot be used any longer to determine the location of the roughening line numerically (as we did in Fig. 10). We would have to use ratios; e.g.,

$$N\eta^+(2)/N\eta^-(1)=4$$

or

$$N\eta^+(1)/N\eta^-(1)=1 .$$

The latter yields trivially the line $D=0$ for all N because of the symmetry relation just stated.

F. Quantum fluid with long-range AF spin order

It is surprising that a fluid can sustain long-range AF spin order in the presence of only short-range interactions. The AF spin interaction is short ranged. Outside this range the particles do not have any energetic preference for AF spin order. The long-range AF spin order is stabilized by a combination of the kinetic energy and short-range repulsion between parallel spins. The particles collide often enough that they prefer that their spins are AF ordered. This is the direct analog of our entropy argument. The spins prefer the AF ordered state because that gives them more positional entropy (zero point motion); see Sec. II B and Fig. 5.

Recall the more detailed argument for the presence of long-range order in the DOF phase in Sec. II. We described the positional and spin-$\frac{1}{2}$ degrees of freedom in terms of Ising and six-vertex degrees of freedom. We found that the presence of an infinitely large backbone in the ensemble of six-vertex lattices is essential for sustaining long-range AF spin order. Systems on finite lattices cannot maintain long-range order and a spontaneous broken symmetry. This backbone lattice represents a collection of intertwining spin-$\frac{1}{2}$ particle world lines that spans the entire space-time in the path integral. Particles at opposite sites of the chain communicate with each other (although in between them particle pairs are being created and annihilated all the time). Information of the collective choice of the preferred spin direction is transferred across the chain by a sequence of advanced and retarded collisions.

G. An exact soluble line

Finally, consider the multicritical point M; see Figs. 2 and 13. The central charge at this point is $c=1.5$ because it represents a simple Ising transition ($c=0.5$) superimposed on a roughening transition ($c=1.0$). This point has been identified with the Wess-Zumino-Witten model by Haldane and Affleck.[33] It is noteworthy in this context that the RSOS model, i.e., the spin-1 chain with discretized time, contains the exactly soluble 19-vertex model solved by Zamolodchikov and Fateev.[34] The interesting aspect of this exact solution is that the exactly soluble subspace lies inside the surface of AF Ising-type critical points. Moving through the exactly soluble subspace is like moving along the line A-S-M-N in Figs. 2 and 13. This path crosses multicritical points of type M and N, but without a singularity in the free energy at point M.[12,24]

V. THE VBS STATE IN THE SPIN-1 CHAIN

A. The VBS state

Recently, Affleck *et al.*[3] showed that at a specific point of the phase diagram of the spin-1 quantum chain the exact ground state is a valence bond solid (VBS) state. Furthermore, this point is close to the Heisenberg (HAF) point, and therefore they suggest that also at the HAF point the ground state is described approximately by the VBS state.

In the preceding section we showed that the HAF point lies inside the DOF phase from the perspective of crystal surface roughening. Now we will demonstrate that the exactly soluble VBS point is part of the DOF phase as well. We will find that the VBS ground state has exactly the type of long-range order and disorder that we

associate with the DOF phase. Moreover, we will demonstrate that at this point the AF spin order is perfect and that the positional disorder is maximal. This suggests that the exactly soluble VBS point plays the role of fixed point of the DOF phase, that in renormalization transformations the VBS point in the phase diagram serves as the sink of the RT flow inside the DOF phase.

Affleck *et al.*[3] represent the VBS state as follows. They express the spin-1 variables as a sum of two spin-$\frac{1}{2}$ variables. Let $\psi_{\alpha\beta}$ denote a spin-1 state in terms of symmetrized spin-$\frac{1}{2}$ variables, i.e.,

$$\begin{aligned}\psi_{++}&=|++\rangle\ ,\\ \psi_{+-}&=\psi_{-+}=(|+-\rangle+|--\rangle)/\sqrt{2}\ ,\\ \psi_{--}&=|--\rangle\ .\end{aligned}\tag{5.1}$$

In the VBS state each spin-$\frac{1}{2}$ is contracted with a spin-$\frac{1}{2}$ at a neighbor site into a singlet state, a so-called valence bond. Define the antisymmetric tensor $\epsilon^{\alpha\beta},\epsilon^{++}=\epsilon^{--}=0$ and $\epsilon^{+-}=-\epsilon^{-+}=1$. Contractions of two spin-$\frac{1}{2}$ variables into a singlet state can be written as $2^{-1/2}\epsilon^{\alpha\beta}|\alpha\beta\rangle$, where summation over repeated indices is implied. The contractions are chosen such that every spin-1 is connected to both its neighbors by a valence bond. The VBS state can be written as

$$\begin{aligned}|\psi_{\rm VBS}\rangle=2^{-N/2}&\psi_{\alpha_1\beta_1}\epsilon^{\beta_1\alpha_2}\psi_{\alpha_2\beta_2}\epsilon^{\beta_2\alpha_3}\cdots\psi_{\alpha_i\beta_i}\\ &\times\epsilon^{\beta_i\alpha_{i+1}}\cdots\psi_{\alpha_N\beta_N}\epsilon^{\beta_N\alpha_1}\ ,\end{aligned}\tag{5.2}$$

where periodic boundary conditions are implied.

Affleck *et al.*[3] show that this state is the ground state for the Hamiltonian

$$H=\sum_n \tfrac{1}{2}\mathbf{S}_n\cdot\mathbf{S}_{n-1}+\tfrac{1}{6}(\mathbf{S}_n\cdot\mathbf{S}_{n-1})^2+\tfrac{1}{3}\ .\tag{5.3}$$

This Hamiltonian is equivalent to the sum of projection operators that project onto the spin-2 contribution for every pair of nearest-neighbor spins,

$$H=\sum_n \tfrac{1}{24}(\mathbf{S}_n+\mathbf{S}_{n+1})^2[(\mathbf{S}_n+\mathbf{S}_{n+1})^2-2]\ .\tag{5.4}$$

We refer to the papers by Affleck *et al.*[3] and Arovas *et al.*[4] for more details.

B. Noninteracting lattice gas with perfect AF spin order

Notice that the hopping probability is negative in Eq. (5.3). To make contact with the HAF point in Fig. 13 we need to make the hopping probability positive. This is achieved by a rotation $S_n^{x,y}\rightarrow -S_n^{x,y}$, $S_n^z\rightarrow S_n^z$ at every odd site n. Consider a section $\epsilon^{\beta_2\alpha_3}\psi_{\alpha_3\beta_3}\epsilon^{\beta_3\alpha_4}$ of the VBS state. For $\alpha_4=\beta_2=\pm$ the spin is in the $S^z=\pm1$ state and the two ϵ contribute a plus sign. For $\alpha_4=-\beta_2=\pm$ the spin is in the $S^z=0$ state and the two ϵ contribute a minus sign. The spin rotation transforms this into a plus sign because the rotation is equivalent to assigning a minus sign to the $S^z=0$ state; see Eq. (5.1). The rotation is therefore equivalent to symmetrizing the tensors at both sides of each rotated spin, $\epsilon^{++}=\epsilon^{--}=0$ and $\epsilon^{+-}=\epsilon^{-+}=1$. For even chain lengths N all ϵ's become symmetric. For odd chain lengths one antisymmetric tensor remains. Its location is arbitrary by gauge invariance.

Under the rotation the Hamiltonian in Eq. (5.3) transforms into the form

$$\begin{aligned}H=\sum_n &\tfrac{2}{3}+\tfrac{5}{12}S_n^zS_{n+1}^z+\tfrac{1}{4}(S_n^zS_{n+1}^z)^2-\tfrac{1}{3}(S_n^z)^2-\tfrac{1}{4}(S_n^+S_{n+1}^-+S_n^-S_{n+1}^+)+\tfrac{1}{24}[(S_n^+S_{n+1}^-)^2+(S_n^-S_{n+1}^+)^2]\\ &-\tfrac{1}{12}[S_n^zS_{n+1}^z(S_n^+S_{n+1}^-+S_n^-S_{n+1}^+)+(S_n^+S_{n+1}^-+S_n^-S_{n+1}^+)S_n^zS_{n+1}^z]\ .\end{aligned}\tag{5.5}$$

Compare this with Eq. (3.6). The two dynamical processes associated with the particle density (particle hopping and particle-pair creation and annihilation) obtain positive probabilities. The third dynamical process, spin exchange, retains its negative probability. Therefore the VBS point remains in a region of the phase diagram of the RSOS model with negative Boltzmann weights.

The spin rotation has simplified the VBS state. The cumbersome signs, associated with the antisymmetric nature of VBS state, have vanished. Diagrammatically we can represent the VBS state now as follows: denote a $S_n^z=+1$ state by a pair of plus signs $(++)$, the $S_n^z=-1$ state by two minus signs $(--)$, and the $S_n^z=0$ state by a plus minus pair $(+-)$. The VBS state is the superposition of all possible states with a $(++)$, $(+-)$, or $(--)$ at each site such that every $+$ is matched by a $-$ at the nearest-neighbor site. These are the valence bonds. Figure 15 shows an example of such a state.

This matching rule implies that a $(++)$ must be followed by a $(--)$, immediately or after an intermediate string of $(+-)$'s. In other words, a particle with an up spin, $S^z=+1$ (a up step in the crystal surface interpretation), must be followed by a particle with a down spin, $S^z=-1$ (a down step). The AF spin order of particles is perfect, but the distance between particles, represented by the length of the string of intermediate $S_n^z=0$, is arbitrary. This is exactly the type of long-range AF spin order and positional disorder that we associate with the DOF phase.

The VBS state can be written as

$$|\psi_{\rm VBS}\rangle=\sqrt{2}|000\ldots\rangle + \sum_{M=2,4,6,\ldots} 2^{M/2} \sum_{\text{permuations}} |011001\ldots\rangle \ , \tag{5.6a}$$

with

$$\sqrt{2}|011001\ldots\rangle=|0\uparrow\downarrow 00\uparrow\ldots\rangle+|0\downarrow\uparrow 00\downarrow\ldots\rangle \ , \tag{5.6b}$$

where 1 (0) denotes an occupied (empty) site, i.e., $S_n^z=\pm 1$ ($S_n^z=0$). The first summation is over occupation numbers, $M=2,4,6,\ldots,N$. The occupation number must be even because the spins of the particles have perfect AF order, and we assume periodic boundary conditions. The second summation is over all possible configurations of the M occupied sites. Each configuration represents two different spin states because the AF spins order is twofold degenerate [see Eq. (5.6b)]. Each particle ($S_n^z=\pm 1$) has a fugacity $\sqrt{2}$. This originates from the $\sqrt{2}$ normalization of the $\psi_{\alpha_n\beta_n}$ in Eq. (5.1). The vacuum, $M=0$, has an anomalous weight 2, because then a $(+,-)$ is located at each site, and it is possible to link them in two ways.

Equation (5.6) applies to even chain lengths. For even values of N all the ϵ tensors become symmetric under the spin rotation discussed above, but for odd chain lengths one tensor remains antisymmetric. For odd values of N the VBS state can be written as

$$|\psi_{\rm VBS}\rangle= \sum_{M=2,4,6,\ldots} 2^{M/2} \sum_{\text{permuations}} |011001\ldots\rangle \ , \tag{5.7a}$$

with

$$\sqrt{2}|011001\ldots\rangle=|0\uparrow\downarrow 0\|0\uparrow\ldots\rangle-|0\downarrow\uparrow 0\|0\downarrow\ldots\rangle \ . \tag{5.7b}$$

The vacuum contribution has disappeared because its two terms now have opposite signs, and cancel. Also the two spin states in Eq. (5.7b) have opposite signs. The location of the remaining antisymmetric ϵ is denoted by $\|$. Its location is gauge invariant, but must be selected to specify a sign convention: the sign is $+$ $(-)$ when the first $S^z\neq 0$ to the right of $\|$ is $S^z=1$ ($S^z=-1$).

It is easy to check by substitution that Eq. (5.6) is indeed an eigenstate of Eq. (5.5). The proof and formulation by Affleck *et al.*[3] using Eq. (5.3), and also by Arovas *et al.*[4] (they use the Schwinger boson formalism), are mathematically more elegant, but Eq. (5.6) has another advantage. It shows most clearly that the VBS state has the properties of a noninteracting lattice gas. This explains the extremely short correlation length in the VBS state. For example, the norm of the VBS state is identical to the partition function of a noninteracting lattice gas with fugacity $z=2$,

$$\langle\psi_{\rm VBS}|\psi_{\rm VBS}\rangle=2+\sum_{M=2,4,6,\ldots} 2^M \begin{bmatrix} N \\ M \end{bmatrix} = \tfrac{1}{2}(3^N+3) \ , \tag{5.8a}$$

for even chain lengths N, and

$$\langle\psi_{\rm VBS}|\psi_{\rm VBS}\rangle= \sum_{M=2,4,6,\ldots} 2^M \begin{bmatrix} N \\ M \end{bmatrix} = \tfrac{1}{2}(3^N-3) \ , \tag{5.8b}$$

for odd chain lengths N.

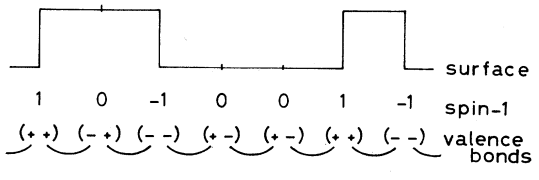

FIG. 15. Typical (side view) configuration in the DOF phase for the RSOS model, as seen from, respectively, the crystal surface, spin-1, and VBS perspective.

C. Order parameters and mass gaps

The preceeding property makes it very easy to calculate all the correlation functions associated with the order and disorder of the DOF phase defined in the preceding sections. Affleck *et al.*[3] have already calculated most of these correlation functions. In our lattice-gas formulation the calculation becomes completely trivial. For simplicity we present the calculation for even chain lengths only.

Define the following sums,

$$Z_0(N)= \sum_{M=0,2,4,\ldots} 2^M \begin{bmatrix} N \\ M \end{bmatrix} \ , \qquad Z_1(N)= \sum_{M=1,3,5,\ldots} 2^M \begin{bmatrix} N \\ M \end{bmatrix} \ . \tag{5.9}$$

Using the binomial expansion,

$$P(a,b)=(a+b)^N= \sum_{M=0,1,2,3,\ldots,N} a^M b^{N-M} \begin{bmatrix} N \\ M \end{bmatrix} \ , \tag{5.10}$$

these sums can be evaluated trivially:

$$Z_0(N)=[P(2,1)+P(-2,1)]/2=[3^N+(-1)^N]/2 \qquad Z_1(N)=[P(2,1)-P(-2,1)]/2=[3^N-(-1)^N]/2 \ . \tag{5.11}$$

In the VBS state the expectation values for finding a particle or a vacancy are equal to

$$\langle 0|(S_n^z)^2|0\rangle=\frac{2Z_1(N-1)}{Z_0(N)+1}=\frac{2}{3} \ , \qquad \langle 0|[1-(S_n^z)^2]|0\rangle=\frac{Z_0(N-1)}{Z_0(N)+1}=\frac{1}{3} \ . \tag{5.12}$$

The probability of finding particles with parallel spins

at site n_0 and site n_0+n with an odd number of particles in between them, $P_{\mathrm{F,odd}}(n)$, and the probability of finding particles with opposite spins at site n_0 and site n_0+n with an even number of particles in between them, $P_{\mathrm{AF,even}}(n)$, are equal to

$$\begin{aligned} P_{\mathrm{F,odd}}(n) &= \frac{4Z_1(n-1)Z_1(N-n-1)}{Z_0(N)+1} \\ &= \tfrac{2}{9}[1+(-1)^n 3^{-n+1}] , \\ P_{\mathrm{AF,even}}(n) &= \frac{4Z_0(n-1)Z_0(N-n-1)}{Z_0(N)+1} \\ &= \tfrac{2}{9}[1-(-1)^n 3^{-n+1}] , \end{aligned} \tag{5.13}$$

in the limit $N\to\infty$. The arrows in the VBS state have perfect AF order; therefore $P_{\mathrm{F,even}}(n)=0$ and $P_{\mathrm{AF,odd}}(n)=0$.

The particle density-density and spin-spin correlation functions, can be expressed in these four probabilities. The density-density correlation function is equal to

$$\begin{aligned} \langle 0|[S^z_{n_0}S^z_{n_0+n}]^2|0\rangle &= P_{\mathrm{F,even}}(n)+P_{\mathrm{AF,odd}}(n) \\ &\quad +P_{\mathrm{F,odd}}(n)+P_{\mathrm{AF,even}}(n)=\tfrac{4}{9} . \end{aligned} \tag{5.14}$$

This is simply the square of the particle density, Eq. (5.12), and confirms that the particle positions are completely uncorrelated. The spin-spin correlation function is equal to

$$\begin{aligned} \langle 0|S^z_{n_0}S^z_{n_0+n}|0\rangle &= P_{\mathrm{F,even}}(n)-P_{\mathrm{AF,odd}}(n) \\ &\quad +P_{\mathrm{F,odd}}(n)-P_{\mathrm{AF,even}}(n) \\ &= \tfrac{4}{3}(-1)^n 3^{-n} . \end{aligned} \tag{5.15}$$

So the order parameter m_s [see Eq. (4.7)] is equal to zero, as expected. The correlation length is extremely short, $\xi=1/\ln(3)$, which is not surprising given the lack of interactions in this lattice-gas-type state.

The fact that the spin-spin correlation decays to zero at large distances, might mislead one to believe that the VBS state lacks long-range spin order. This correlation function mixes positional and spin-type order (see Sec. IV C). To exhibit the AF spin order of the particles properly you must consider the correlation function $G_s(n)$ in Eq. (4.5). $G_s(n)$ can be expressed in the above four probabilities too;

$$\begin{aligned} G_s(n) &= P_{\mathrm{F,even}}(n)+P_{\mathrm{AF,odd}}(n)-P_{\mathrm{F,odd}}(n) \\ &\quad -P_{\mathrm{AF,even}}(n)=\tfrac{4}{9} . \end{aligned} \tag{5.16}$$

The absence of any distance dependence illustrates that the AF spin order is perfect. The spin-type order parameter ψ of the DOF phase, see Eq. (4.4), is equal to $|\psi|=\frac{2}{3}$. This is simply the probability to find the site occupied; see Eq. (5.12).

The probability of finding an even and an odd number of particles between sites n_0 and n_0+n is equal to

$$\begin{aligned} P_{\mathrm{even}}(n) &= \lim_{N\to\infty}\frac{Z_0(n)Z_0(N-n)+1}{Z_0(N)+1}=\tfrac{1}{2}[1+(-1)^n 3^{-n}] , \\ P_{\mathrm{odd}}(n) &= \lim_{N\to\infty}\frac{Z_1(n)Z_1(N-n)}{Z_0(N)+1}=\tfrac{1}{2}[1-(-1)^n 3^{-n}] . \end{aligned} \tag{5.17}$$

The correlation function $G_H(n)$, defined in Eqs. (2.4) and (4.2), couples to the parity of the column heights in the crystal surface (see Sec. II E) and is equal to

$$G_H(n)=P_{\mathrm{even}}-P_{\mathrm{odd}}=(-1)^n 3^{-n} . \tag{5.18}$$

This correlation function decays to zero at large distances. The Ising spin magnetization ρ [see Eq. (4.3)] is equal to zero. This illustrates once more that the VBS point belongs to the DOF phase, and not to the RSOS flat phase (the disordered singlet phase). In the latter ρ is nonzero (see Sec. II E).

It is also easy to calculate the interface free energies $\eta^{\pm}(a)$ defined in Secs. II and IV. Consider the ground-state energies $E_0^{\pm}(a)$ for periodic and antiperiodic boundary conditions ($S^z_n=\pm S^z_{n+N}$) with magnetization $a=0,1$. Recall the definition $\eta^{\pm}(a)=E_0^{\pm}(a)-E_0^{+}(0)$.

The $(-,1)$ boundary condition does not impose a topological frustration onto the AF spin order [see Fig. 9(d)]. The exact ground state for the $(-,1)$ boundary condition is again a VBS state. This VBS state contains an odd number of particles:

$$|\psi_{\mathrm{VBS}}\rangle = \sum_{M=1,3,5,\ldots} 2^{M/2} \sum_{\text{permuations}} |011001\ldots\rangle , \tag{5.19a}$$

with

$$\sqrt{2}|011001\ldots\rangle = |0\uparrow\downarrow 0\|0\downarrow\ldots\rangle + |0\downarrow\uparrow 0\|0\uparrow\ldots\rangle , \tag{5.19b}$$

with $\|$ the seam across which the particles see each other with reversed spin. This state has the same energy as the VBS state for the $(+,0)$ boundary condition, Eq. (5.6). Therefore $E_0^-(1)=E_0^+(0)$, not only in the thermodynamic limit, but also for all finite N. This confirms, see Eq. (2.9), that the mass of the particles and vacancies, η_I^F and η_I^{AF}, are indeed equal to zero.

We are not aware of any simple form of the ground state for the $(+,1)$ and $(-,0)$ boundary conditions. Numerically, by solving finite chains up to $N=10$ we find that $E_0^+(1)$ and $E_0^-(0)$ differ slightly, but become rapidly identical in the thermodynamic limit. This is expected, because the soliton sees itself repeated over a distance N for the $(+,1)$ boundary condition, but it sees itself reversed for the $(-,0)$ boundary condition (an $\uparrow\uparrow$ pair sees a $\downarrow\downarrow$ pair). The soliton must have finite width, because the correlation length inside the DOF phase is finite. Therefore $E_0^+(1)$ must become equal to $E_0^-(0)$ in the limit of infinite chain length. By extrapolation of the numerical results for $N=2,4,\ldots,12$ we find that the Néel soliton mass is equal to $\eta^+(1)=\eta^-(0)=2.100\,66$.

D. Role of the VBS point in the DOF phase

These results demonstrate that the positional disorder of the particles and also their AF spin order are both perfect at the VBS point. This suggests that the VBS state can be used as the archetype state to describe the DOF phase and these VBS fluids. The VBS point then plays the role of fixed point of the DOF phase in RT transformations. The HAF point and the Hamiltonian (5.1) are invariant under global spin rotations, while the general Hamiltonian, Eq. (3.6) lacks this symmetry [to be precise, it lacks the modified version of the rotational invariance that applies after the spin rotation at all odd sites that we used to transform Eq. (5.2) into Eq. (5.6)]. If the VBS state is indeed the fixed point of the DOF phase, then the entire DOF phase must have this global rotational invariance at large length scales, and this type of rotational symmetry breaking must be an irrelevant operator. This is somewhat surprising because this symmetry does not play any role in our description of the DOF phase in Secs. II and IV.

VI. INTEGER VERSUS HALF-INTEGER SPIN CHAINS

A. Ground state degeneracy in the spin-1 chain

The RSOS flat phase and the DOF phase behave quite normally in the RSOS representation of the model. Both have long-range order, a spontaneously broken symmetry, a ground-state degeneracy, and local order parameters. In both phases the translation symmetry in the column height direction, orthogonal to the surface, $h \rightarrow h+1$, is spontaneously broken. In the RSOS flat phase the average height is an integer and in the DOF phase a half-integer.

The RSOS flat phase also behaves quite normally in the spin-1 representation of the model. Recall that the steps represent the world lines of the spins in the quantum chain. The information about the absolute height of the crystal surface is lost when the surface configuration is represented in terms of steps instead of column heights. Therefore the RSOS flat ground state is nondegenerate in the spin-1 formulation. This is no surprise. In the spin-1 language the RSOS flat phase is interpreted as a disordered dilute gas phase (a disordered singlet phase). Therefore no ground-state degeneracy is expected. The order operator of the RSOS model becomes a familiar type of disorder operator.

However, the same happens in the DOF phase. There it leads to confusion. In the spin-1 representation the DOF phase obtains the unusual property that it displays long-range AF spin order, but without a spontaneously broken symmetry nor a ground-state degeneracy. The VBS phase does not represent a disordered fluid; it has long-range order. This is one of the central issues in the fractional quantum Hall effect[5] and also, as we will see in the following, the Haldane conjecture. Therefore we want to discuss this effect in detail. VBS phases in general and also the Laughlin wave function for the fractional quantum Hall effect represent fluid-type states that on one hand are disordered but on the other hand carry massive soliton type topological excitations with fractional topological charge. In our case the positional disorder of the spin-$\frac{1}{2}$ particles implies the fluid character, and the Néel solitons associated with the long-range AF spin order are the carriers of topological fractional charge ($q=\frac{1}{2}$).

We found in Sec. IV that the order parameters ρ and ψ, that distinguish between the RSOS flat and the DOF phase, cannot be expressed as an expectation value in terms of spin-1 operators alone. The parity of the crystal column height at the seam between sites N and 1, $\exp(i\pi h_0)$, must be included to distinguish their sign. See Eqs. (4.1)–(4.6). Only then does the DOF phase maintain its ground-state degeneracy and broken symmetry in the spin-1 formulation. Only with h_0 included is the mapping of the column height configurations to spin configurations one to one. Recall that h_0 changes as $h_0 \rightarrow h_0 \pm 1$ each time a spin-$\frac{1}{2}$ particle crosses the seam or when a particle pair is being created or annihilated at the seam.

It is instructive to discuss the issue of spontaneous symmetry breaking from the BCSOS flat phase perspective. The AF ground state is twofold degenerate; call them state A and B. Every site is occupied by a spin-$\frac{1}{2}$ particle, and these spins are perfectly AF ordered. The order parameters have the values $m_s=\pm 1$, $\rho_s=1$ (if h_0 is even), and $\psi=\pm 1$ [see Eqs. (4.1)–(4.6)]. Consider the usual Peierls argument: the presence of spontaneous symmetry breaking implies that several sectors in phase space do not communicate with each other by thermodynamic (quantum) fluctuations; they are separated by infinite (free) energy barriers. There are two types of processes by which state A can transform into B.

(a) Create a Néel soliton pair, i.e., an $\uparrow\uparrow$ and a $\downarrow\downarrow$ interface across the entire lattice in the timelike direction (compare with Fig. 9). Move one of them around the cylinder one time and then let it recombine with the other soliton. This process transforms state A into B but does not change h_0: $\psi \rightarrow -\psi$, $\rho_s \rightarrow \rho_s$, and $m_s \rightarrow -m_s$.

(b) The same can be achieved by creating a hole-type soliton pair, and repeating the same process. Again A transforms into B, but now h_0 changes, $h_0 \rightarrow h_0 \pm 1$. Therefore $\psi \rightarrow \psi$, $\rho_s \rightarrow -\rho_s$, and $m_s \rightarrow -m_s$.

The Néel soliton mass $\eta_s^+(1)$ is associated with process (a) and the mass of a hole-type interface η_I^{AF} with (b). Both are finite in the BCSOS flat phase. Both processes encounter infinite (free) energy barriers in the thermodynamic limit, respectively, $N_t \eta_s^+(1)$ and $N_t \eta_I^{\mathrm{AF}}$. Therefore ψ, ρ_s, and m_s are nonzero in the BCSOS flat phase.

The Néel soliton mass $\eta_s^+(1)$ vanishes at the roughening line (see Figs. 2 and 13). Therefore ψ and m_s are zero in the BCSOS rough phase, but ρ_s remains finite. On the other hand, the mass of the holes η_I^{AF} vanishes at the AF Ising critical line. Therefore ρ_s and m_s vanish in the DOF phase, but ψ remains finite. Notice that not only the DOF phase but also the massless BCSOS rough phase has a ground-state degeneracy and broken symmetry.

These ground-state degeneracies disappear when we ignore h_0. Only the ground-state degeneracy of the BCSOS flat phase remains. We can calculate still the absolute

values of the order parameters ψ and ρ, but not their sign. The ground-state degeneracy associated with them is lost. The order parameter m_s is the only one whose sign can be determined. In the DOF phase the spins of the spin-$\frac{1}{2}$ particles have long-range AF order. Process (a), which changes the sign of ψ, still encounters an infinite free-energy barrier, but without h_0 we cannot distinguish between process (a) and (b). All the AF ordered spin states can fluctuate into each other by movements of the particles without ever flipping any spin, process (b). They can move freely because the DOF phase is a fluid; the hole and particle masses η_I^{AF} and η_I^{F} are zero. Then, following Peierls' argument the ground state cannot be degenerate.

The ground state is obviously degenerate in a "moving frame of reference," where you ride on top of one of the spin-$\frac{1}{2}$ particles. On average the spin of each specific particle is nonzero. This is consistent with the preceding result because to transform from the stationary frame of reference to the moving one you need to evoke h_0 again. To recognize whether a stationary state belongs to phase A or B you need to keep track of the position of your particle in the chain. You need to know whether there are an odd or even number of particles in the chain between your particle and the seam. The variable $\exp(i\pi h_0)$ keeps track of this because it changes sign each time a particle moves across the seam, or when a particle pair is being created and/or annihilated at the seam. Thus it is no surprise that in the moving frame of reference you reintroduce spontaneous symmetry breaking.

B. The Haldane conjecture

Let's turn now to the Haldane conjecture and quantum spin chains in general. In Sec. III we showed in detail that the quantum spin-1 chain is equivalent to the restricted solid-on-solid (RSOS) model. In the RSOS model the step heights in the crystal surface are restricted to $\delta h = 0, \pm 1$. More generally, spin-s quantum chains, with integer s, are equivalent to solid-on-solid models where the step heights are restricted to $|\delta h| \leq s$. In complete analogy to the spin-1 chain, the spin-s chain can be thought of as describing a gas of spin-$(s-\frac{1}{2})$ particles. The steps in the crystal surface play again the role of the world lines of these spin-$(s-\frac{1}{2})$ particles and the absence of a step represents again an empty site. DOF phases are present in SOS models, in general, and therefore also in integer-spin chains, in general.

The Haldane conjecture is often interpreted as stating that "the Heisenberg AF chain for integer spins is massive, while for half-integer spins it is massless." This is incorrect. It suggests that integer and half-integer spin chains differ in a fundamental way and suggests that DOF flat phases can only be realized in integer spin chains. The latter contradicts physical intuition. Half-integer spin chains are equivalent to body-centered solid-on-solid (BCSOS) models (see Sec. III C), and describe surfaces with a body-centered type of symmetry [like Ni(110) and Cu(110)]. There is no reason to expect that such surfaces cannot include a DOF phase.

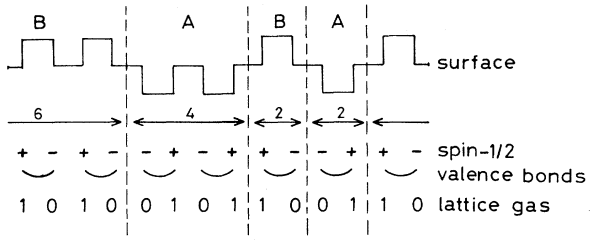

FIG. 16. Typical (side view) configuration in the DOF phase, for the BCSOS model, as seen from, respectively, the crystal surface, spin-$\frac{1}{2}$, VBS, and lattice-gas perspective. Notice that the distances between alternating up and down steps must be even.

C. DOF phases in body-centered-type surfaces

The atoms in the next layer of body-centered surfaces are not placed on top of the atoms in the previous layer but instead above the centers of the plaquettes; see Fig. 6. In the BCSOS model this is modeled by demanding that nearest-neighbor columns of atoms differ in height by an odd integer: $\delta h = \pm 1, \pm 3, \ldots, 2s$. The column height h is even on one sublattice and odd on the other: $\delta h = 0$ is excluded. The low-temperature flat phase is corrugated. It is represented by the AF ordered spin state, $S_n^z = (-1)^n \frac{1}{2}$. So, unlike the spin-1 case, the flat phase remains twofold degenerate.

The mechanisms responsible for surface roughening and the DOF phase are not affected by this surface corrugation. It washes out at large length scales. But a few details change. They all have to do with this remaining twofold degeneracy of the flat phase of the BCSOS model in the spin-$\frac{1}{2}$ representation.

Steps in the crystal surface are now composite objects. They correspond to excitations with two parallel nearest-neighbor spins. These objects have long-range AF order in the DOF phase. An $\uparrow\uparrow$ spin pair will be followed by an $\downarrow\downarrow$ spin pair. Figure 16 shows a typical DOF configuration for the spin-$\frac{1}{2}$ chain. As before, these steps are positionally disordered, i.e., the length of the intermediate string of perfectly ordered AF spins is arbitrary.

Half-integer spin chains are massless at the HAF point according to the preceeding of the Haldane conjecture. This belief is mostly based on the exactly soluble spin-$\frac{1}{2}$ chain. The exact solution includes only the BCSOS flat and BCSOS rough (massless) phase. The Heisenberg AF point coincides actually with the KT transition point between these two phases.[8] It is no surprise that the exact solution does not include a DOF phase. The model only includes nearest-neighbor interactions between the spins. This is not enough to stabilize the DOF phase because (unlike integer-spin chains) the steps are composite objects (pairs of parallel spins). Following our discussion in Sec. II, the model lacks an interaction which favors two parallel up spins to be followed by two parallel down spins. There is no doubt that the DOF phase must become stable in half-integer spin chains, when we increase the range of the interactions. The entropy argument in Sec. II and Fig. 5 is very general.

D. VBS point in the spin-$\frac{1}{2}$ chain

In Sec. V we identified the VBS state in the spin-1 chain as the prototype state describing the DOF phase for integer-spin chains. In the spin-$\frac{1}{2}$ chain there is a similar exactly soluble point. Majumdar and Ghosh,[9] see also Affleck *et al.*,[3] showed that the ground state of the Hamiltonian

$$H=\sum_n [\tfrac{4}{3}\mathbf{S}_n\cdot\mathbf{S}_{n+1}+\tfrac{2}{3}(\mathbf{S}_n\cdot\mathbf{S}_{n+2})^2+\tfrac{1}{2}] \tag{6.1}$$

is a valence-bond state. The Hamiltonian is a sum over projection operators that project onto spin-$\frac{3}{2}$ (see Affleck *et al.*[3]). This Hamiltonian has the Heisenberg AF rotation symmetry. Every spin forms a valence-bond state with one of its neighbors. The ground state

$$|\psi_{\rm VBS}\rangle=2^{-N/2}\psi_{\alpha_1}\epsilon^{\alpha_1\alpha_2}\psi_{\alpha_2}\otimes\cdots\otimes\psi_{\alpha_n}\epsilon^{\alpha_n\alpha_{n+1}}\psi_{\alpha_{n+1}}\otimes\cdots\otimes\psi_{\alpha_{N-1}}\epsilon^{\alpha_{N-1}\alpha_N}\psi_{\alpha_N} \tag{6.2}$$

has a dimerized-type twofold degeneracy, as shown schematically in Fig. 16.

Just like the spin-1 case, this VBS state is the prototype DOF state. The discussion is completely parallel but more simple than for the spin-1 model. Again, perform the rotation $S_n^{x,y}\rightarrow -S_n^{x,y}$, $S_n^z\rightarrow S_n^z$, at the odd sites, to get rid of the antisymmetric nature of the valence bonds. Then also this VBS state obtains the character of a noninteracting lattice gas: $S_n^z=\frac{1}{2}$ ($S_n^z=-\frac{1}{2}$) represent occupied (empty) sites; the particle density is fixed such that the chain is half filled, $M=N/2$; and the particles do not interact, except for the constraint that at least one of the sites next to every vacant site must be occupied and at least one of the sites next to every occupied site must be vacant. The latter condition implies that the steps, i.e., the occurance of bonds with both sites occupied (an up step, $\uparrow\uparrow$ excitation) or empty (a down step, $\downarrow\downarrow$ excitation), are completely randomly placed, except that they all occur at even distances from each other, and that up and down steps occur in strict alternating order. As before, the positional disorder of the steps and their AF up-down order are both perfect. Also this VBS point belongs to the DOF phase, and again it most likely plays the role of the fixed point of the entire DOF phase of the spin-$\frac{1}{2}$ chain.

So contrary to what the commonly used but incorrect formulation of the Haldane conjecture suggests, it cannot mean to exclude DOF phases from half-integer spin chains. DOF phases occur in integer and half-integer spin chains alike. What does it say?

E. Ground-state degeneracy in the spin-$\frac{1}{2}$ chain

Affleck and Lieb[35] have given a "proof" of the Haldane conjecture. They show that in half-integer spin chains only two types of phases can be realized: (i) phases without a degenerate ground state must be massless, and (ii) phases with a mass gap must have a degenerate ground state. This excludes phases with a mass gap that lack a ground-state degeneracy, such as the RSOS flat phase in the spin-1 chain, and, more importantly, also the DOF phase in the spin-1 chain. However, this result does not exclude DOF phases in half-integer spin chains. We just found that the absence of a broken symmetry in DOF phases in integer spin chains is a peculiarity of the spin formulation. It has a genuine spontaneous symmetry breaking in the surface roughening formulation. We will find that the only difference between DOF phases in integer and half-integer spin chains is that in half-integer spin chains the DOF phase retains some of its ground-state degeneracy when we translate from the BCSOS formulation to the spin-$\frac{1}{2}$ formulation.

In analogy with the RSOS model, the translational symmetry in the direction orthogonal to the surface is broken in both the flat and DOF phases of the BCSOS model, $h\rightarrow h+1$, with a half integer and integer average height, respectively. However, in the BCSOS model this translational symmetry must be accompanied by a translation along the surface, i.e., $h_{\mathbf{r}}\rightarrow h_{\mathbf{r}'}+1$ with $\mathbf{r}=(x,y)$ and $\mathbf{r}'=(x+1,y)$ because the column heights can only be even or odd on each sublattice.

In the spin-$\frac{1}{2}$ formulation the flat phase remains twofold degenerate; call them phases A and B. Suppose that the column between sites N and 1 (the seam) belongs to the sublattice where the column height h_0 is even. Then, in phase A (B) the average column height in the BCSOS flat phase is $h_0-\frac{1}{2}$ ($h_0+\frac{1}{2}$). Also notice that you automatically switch between phase A and phase B when you cross a step, and that the distance between a neighbor up-step ($\uparrow\uparrow$) and down-step ($\downarrow\downarrow$) pair is even while the distance between up-up or down-down neighbor steps is odd (see Fig. 16).

The steps in the DOF phase are disordered positionally, but they are placed at even distances from each other. So unlike the spin-1 case, information of the parity of the height of the crystal surface is preserved in the spin-$\frac{1}{2}$ representation. The twofold degeneracy of the flat and DOF phase in the spin-$\frac{1}{2}$ representation contains the parity information of the crystal surface height. In integer-spin chains we must include a seam variable, $\exp(i\pi h_0)$, to keep track of the column height parity (Sec. IV). ρ and ψ are nonlocal operators in the spin-1 model, because the only way to keep track of (relative) parity, is by knowing whether you crossed an even or odd number of steps [the string operator in Eqs. (4.2)–(4.6)]. In the spin-$\frac{1}{2}$ chain we do not need this. The spin-$\frac{1}{2}$ algebra keeps track of the parity by itself. The corrugation of the crystal surface acts as a local index that keeps track of the parity of the surface height. Two steps (arbitrarily far apart from each other) have an even (odd) number of steps in between them if the phase directly to the left of them belongs to the same (different) type of phase (A or B). Therefore the order parameters ρ and ψ that distinguish between the flat and DOF phases remain local in the

quantum spin formulation:

$$\rho=\langle(-1)^n S_n^z\rangle \tag{6.3}$$

and

$$\psi=\langle(-1)^n\tfrac{1}{2}(S_n^z S_{n+1}^z+1)\rangle\ . \tag{6.4}$$

F. Conclusion

We found that from the surface roughening perspective there is no fundamental difference between the DOF phase in simple and BC-type surfaces. Also in the quantum spin formulation there is no real difference. The DOF phase in integer spin chains can be interpreted as a fluid of spin-$\frac{1}{2}$ particles with long-range AF spin order. Similarly the $\uparrow\uparrow$ and $\downarrow\downarrow$ excitations with respect to the Néel phase in the spin-$\frac{1}{2}$ chain can be interpreted as spin-$\frac{1}{2}$ particles in their own right (with $\sigma^z=+1$ representing a $\uparrow\uparrow$ and $\sigma^z=-1$ representing a $\downarrow\downarrow$ excitation). The DOF phase in the model is a phase where these particles form a fluid with long-range AF spin order. DOF fluids in integer and half-integer spin chains are stabilized by exactly the same physical mechanism (the entropy argument of Sec. II). The only difference is that because of the composite nature of these particles in the half-integer spin chains, the long-range order of the DOF phase can be expressed in terms of a local order parameter and a degenerate ground state, while in the integer-spin chains the ground-state degeneracy, although trivial in the crystal surface formulation, gets lost in the spin representation.

ACKNOWLEDGMENTS

This research is supported by the National Science Foundation under Grant Nos. DMR 85-09392 and DMR 88-13083.

APPENDIX: THE LOCATION OF THE KT PHASE BOUNDARY IN THE RSOS MODEL

In this appendix we show that the general RSOS model of Eq. (2.1) has a special symmetry in the subspace

$$\exp(-L_2^{(x)})+\exp(-L_2^{(t)})=1\ .$$

The step-1 surface tension with periodic boundary condition $\eta^+(1)$ [see Eq. (2.9)] is equal to the step-1 surface tension with antiperiodic boundary conditions $\eta^-(1)$, along this line for all values of the strip width N. From this observation we conclude that the KT transition must occur in the half space:

$$\exp(-L_2^{(x)})+\exp(-L_2^{(t)})\geq 1\ .$$

This is to the left of the line $\exp(L_2)=2$ in Fig. 2 where the lattice is isotropic, $L_2^{(x)}=L_2^{(t)}$. It is to the left of the line $J=0$ in Fig. 13 because the spin-1 quantum chain is identical to the RSOS model in the limit of a very anisotropic lattice (see Sec. III B). This proves that the Heisenberg AF point does not belong to the massless spin-wave phase (the RSOS and BCSOS rough phases).

In Sec. II we reformulated the RSOS model as a six-vertex model defined on an annealed lattice generated by an Ising model. The intersections of the Ising-Bloch walls serve as the vertices of this annealed lattice, whereas the Bloch walls themselves are the bonds of the lattice. Consider the topological difference between the periodic and antiperiodic step-1 boundary conditions, respectively, $(+,1)$ and $(-,1)$. Compare Figs. 9(b) and 9(d). The difference is that for $(-,1)$ the arrows on the steps must be reversed each time the seam is crossed. We will show that the arrows do not convey any information in the subspace

$$\exp(-L_2^{(x)})+\exp(-L_2^{(t)})=1\ ,$$

and that therefore the ground-state energies for these two boundary conditions are the same.

Consider a certain Ising-Bloch-wall configuration, i.e., a certain six-vertex model lattice. Instead of placing arrows on the bonds of this lattice, consider all possible ways of completly covering it with polygons.[36] Polygons are closed loops that do not intersect, but they meet each other at the Bloch wall intersections. Give each polygon a weight $\sqrt{q}$, and assign a weight z_x respectively z_t to each vertex depending on whether two vertical of two horizontal polygons meet. This leads to the partition function

$$Z=\sum_{\mathcal{N}} q^{N_P/2} z_x^{N_x} x_t^{N_t}\ .$$

The sum is over all polygon configurations $\mathcal{N}$. N_P is the number of polygons in the configuration, and N_x ($N_t=N_V-N_x$) is the number of times polygons meet vertically (horizontally). N_V is the number of Ising-Bloch-wall intersections, i.e., vertices of the six-vertex lattice. There are 2^{N_V} polygon coverings of the Bloch-wall lattice because every possible configuration can be generated by all possible ways of splitting up each Bloch-wall intersection; a loop can choose between turning to the left or right at every intersection point (polygons meet horizontally or vertically).

This problem is intricately related to the Potts model[36] and can be mapped onto the six-vertex model on the same Bloch-wall lattice by assigning arrows to the polygons (either clockwise or counterclockwise). Now the factor $\sqrt{q}$ of each polygon is represented as a local operator by assignment of a phase factor $\beta=\exp(i\mu/4)$ [$\beta^{-1}=\exp(-i\mu/4)$] to each right (left) turn of the polygon in the direction of the arrow (all turns are over 90° because of the underlying square lattice). The parameter μ is related to q as $2\cos(\mu)=\sqrt{q}$ [see Fig. 7(b)]. Vertex states 1–4 correspond in a one-to-one way to a polygon configuration. In state 1 and 2 two vertical polygons meet and in state 3 and 4 two horizontal polygons. Vertex states 5 and 6 are mixtures of both events. They correspond to two different local polygon configurations. See Baxter *et al.*[36] for a detailed account of this mapping, which they considered in the context of the q-state Potts model. It is valid for arbitrary lattice shapes. For general polygon weights $\sqrt{q}$ the model does not coincide

with our six-vertex model, Fig. 7(a), because we assign a weight 1 to turns of the arrowed polygons at nonintersection points of the Bloch walls, states 7 and 8 in Fig. 7(b). However, at $q=4$ ($\mu=0$), the phase factors become equal to 1, and the models coincide in the subspace

$$\exp(-L_2^{(x)})+\exp(-L_2^{(t)})=1 .$$

In this subspace the partition function of our six-vertex model is uniquely determined by the polygons alone, and becomes a so-called two-color oriented nonintersecting string model, which is equivalent to a two-component nonintersecting string model.[37]

The following transformation is a Gauge transformation in this subspace. Draw a closed contour on the lattice and reverse all arrows in the enclosed area, i.e., define the conventional six-vertex model, but with the additional rule that the arrow on each step must be reversed when the step crosses the contour. In general this changes the partition function, but not so in the $\exp(-L_2^{(x)})+\exp(-L_2^{(t)})=1$ subspace. Each polygon intersects the contour an even number of times. All right (left) turns of the arrows are changed into left (right) turns along sections of the polygon inside the contour, but this does not affect the counting of the polygon weight $\sqrt{q}$ by the phase factors because $\mu=0$.

Compare two typical configurations for the periodic and antiperiodic step-1 boundary conditions, Figs. 9(b) and 9(d). None of the polygons to the right of the seam can cross the open step that spans the entire lattice in the timelike direction. Therefore, every polygon intersects the seam an even number of times (except the open step that spans the lattice, but we can take care of that separately). So reversing all arrows between the seam and the open step is a Gauge transformation of the same type as mentioned earlier. The free energy is invariant under this transformation in the subspace

$$\exp(-L_2^{(x)})+\exp(-L_2^{(t)})=1 .$$

The annealed average over the Ising configurations, i.e., all possible six-vertex lattices, does not affect this Gauge symmetry. Thus we proved that $Z(+,1)=Z(-,1)$, i.e., that $\eta^+(1)=\eta^-(1)$. Notice the importance of the presence of the open step in the proof. It excludes automatically configurations with polygons (steps) that wrap around the cylinder. For example, $Z(+,0)\neq Z(-,0)$ because the $(+,0)$ boundary condition allows closed polygons that wrap around the cylinder, while the $(-,0)$ boundary condition (the arrow reversal rule) excludes them.

It is extremely likely that this subspace coincides with the KT roughening transition. This is certainly true in the limit $K\to-\infty$ ($D\to-\infty$), where the six-vertex lattice coincides with the underlying square lattice; we know this from the exact solution.[8] The six-vertex lattice is diluted at finite values of K, but in every configuration the six-vertex model is at its KT critical point; in the aforementioned subspace every six-vertex model maps onto the four-state Potts model at criticality.[36] So the annealed average, Eq. (2.3), is over an ensemble of six-vertex models which are simultaneously at their KT critical point. Therefore the RSOS model should be at its KT critical point as well. The finite six-vertex lattice contributions in the ensemble are noncritical, but their contribution can be estimated using finite-size-scaling arguments, and we expect that they only contribute to the corrections to scaling.

[1]F. D. M. Haldane, Phys. Lett. **93A**, 464 (1983); Phys. Rev. Lett. **50**, 1153 (1983); J. Appl. Phys. **57**, 3359 (1985).

[2]See, e.g., M. P. Nightingale and H. W. J. Blöte, Phys. Rev. B **33**, 659 (1986); H. Schulz and T. Ziman, *ibid.* **33**, 6545 (1986); J. B. Parkinson and J. C. Bonner, *ibid.* **32**, 4703 (1985); J. Solyom and T. Ziman, *ibid.* **30**, 3980 (1984); U. Glaus and T. Schneider, *ibid.* **30**, 215 (1984).

[3]I. Affleck, T. Kennedy, E. H. Lieb, and H. Tasaki, Phys. Rev. Lett. **59**, 799 (1987); Commun. Math. Phys. **115**, 477 (1988).

[4]D. P. Arovas, A. Auerbach, and F. D. M. Haldane, Phys. Rev. Lett. **60**, 531 (1988).

[5]See, e.g., *The Quantum Hall Effect*, edited by R. E. Prange and S. M. Girvin (Springer, New York, 1986).

[6]See, e.g., Physics Today, **41**, (2), 19 (1988).

[7]K. Rommelse and M. P. M. den Nijs, Phys. Rev. Lett. **59**, 2578 (1987).

[8]E. H. Lieb, Phys. Rev. Lett. **18**, 1046 (1967); **19**, 108 (1967).

[9]C. K. Majumdar and D. K. Ghosh, Math. Phys. **10**, 1399 (1969).

[10]S. M. Girvin and A. H. MacDonald, Phys. Rev. Lett. **58**, 1252 (1987); E. H. Rezayi and F. D. M. Haldane, *ibid.* **61**, 1985 (1988); N. Read, *ibid.* **62**, 86 (1989); S. C. Zhang, T. H. Hansson, and S. Kivelson, *ibid.* **62**, 82 (1989).

[11]For a review see J. D. Weeks, in *Ordering in Strongly Fluctuating Condensed Matter Systems*, edited by T. Riste (Plenum, New York, 1980), p. 293.

[12]T. T. Truong and M. P. M. den Nijs, J. Phys. A **19**, L645 (1986).

[13]See, e.g., M. P. M. den Nijs, J. Phys. A **18**, L549 (1985).

[14]F. Gallet, S. Balibar, and E. Rolley, J. Phys. (Paris) **48**, 369 (1987); J. E. Avron *et al.*, Phys. Rev. Lett. **45**, 814 (1980).

[15]J. Villain, D. R. Grempel, and J. Lapujoulade, J. Phys. F **15**, 809 (1985); M. P. M. den Nijs, E. K. Riedel, E. H. Conrad, and T. Engel, Phys. Rev. Lett. **55**, 1689 (1985); **57**, 1279 (1986).

[16]For a review see, M. P. M. den Nijs, in *Phase Transitions and Critical Phenomena* edited by C. Domb and J. L. Lebowitz (Academic, London, 1988), Vol. 12.

[17]H. van Beijeren, Phys. Rev. Lett. **38**, 993 (1977).

[18]M. P. M. den Nijs, Phys. Rev. B **32**, 4785 (1985).

[19]See, e.g., Th. Niemeijer and J. M. J. van Leeuwen, in *Phase Transitions and Critical Phenomena*, edited by C. Domb and M. S. Green (Academic, London, 1976), Vol. 6.

[20]M. P. M. den Nijs (unpublished).

[21]See, e.g., M. P. Nightingale, J. Appl. Phys. **53**, 7927 (1982).

[22]For a review see J. L. Cardy, in *Critical Phenomena and Phase Transitions*, edited by C. Domb and J. L. Lebowitz (Academic, London, 1987), Vol. 11.

[23]H. W. J. Blöte, J. L. Cardy, and M. P. Nightingale, Phys. Rev. Lett. **56**, 742 (1986).

[24]K. Rommelse and M. P. M. den Nijs (unpublished).
[25]M. Kohmoto, M. P. M. den Nijs, and L. P. Kadanoff, Phys. Rev. B **24**, 5229 (1981).
[26]For a review see M. Wortis, in *Chemistry and Physics of Solid Surfaces,* edited by R. Vanselow (Springer-Verlag, Berlin, 1988), Vol. VII, p. 367.
[27]U. Glaus, Physica **141A**, 295 (1987); K. Saitoh, S. Takada, and K. Kubo, J. Phys. Soc. Jpn. **56**, 3755 (1987).
[28]R. J. Baxter, Ann. Phys. **70**, 193 (1972); **70**, 323 (1972).
[29]M. P. M. den Nijs, Phys. Rev. B **23**, 6111 (1981); F. D. M. Haldane, Phys. Rev. Lett. **45**, 1358 (1980).
[30]See, e.g., E. H. Lieb and F. Wu, in *Phase Transitions and Critical Phenomena* edited by C. Domb and M. S. Green (Academic, London, 1972), Vol. 1.
[31]M. P. M. den Nijs, Physica **111A**, 273 (1982).
[32]Recently D. Arovas and S. M. Girvin numerically evaluated our order parameter away from the VBS point; see D. Arovas and S. M. Girvin, Bull. Am. Phys. Soc. **34**, 932 (1989). An early report on our identification of the order parameter was presented in Bull. Am. Phys. Soc. **33**, 797 (1988).
[33]I. Affleck and F. D. M. Haldane, Phys. Rev. B **36**, 5291 (1987).
[34]A. B. Zamolodchikov and V. A. Fateev, Yad. Fiz. **32**, 581 (1980) [Sov. J. Nucl. Phys. **32**, 298 (1980)].
[35]I. Affleck and E. H. Lieb, Lett. Math. Phys. **12**, 57 (1986).
[36]R. J. Baxter, S. B. Kelland, and F. Y. Wu, J. Phys. A **9**, 397 (1976).
[37]J. H. H. Perk and F. Y. Wu, J. Stat. Phys. **42**, 727 (1986).